

MFN= 002658

01 SID/SCD

02 3839

03 INPE-3839-PRE/909

04 CEA

05 S

06 as

10 Batista, Inez Staciarini

10 Abdu, Mangalathayil Ali

10 Bittencourt, Jose Augusto

12 Equatorial f region vertical plasma drifts: seasonal and longitudinal asymmetries in the American sector

14 12055-12064

30 Journal Geophysical Research A

31 91

32 11

40 En

41 En

42 <E>

58 DAE

59 PESQUISA DA IONOSFERA

61 <PI>

64 <1986>

68 PRE

76 AERONOMIA

83 Longitudinal and seasonal asymmetries in the evening ionospheric F region plasma vertical drift (V_z) enhancements, between two longitudinally separated stations situated along the magnetic equator, in the American sector, are investigated under solar maximum conditions, based on results obtained from the analysis of ionosonde data for these stations. The two stations are Huancayo, Peru, and Fortaleza, Brazil, which have markedly different magnetic declination angles. The observed asymmetries are interpreted using a detailed numerical simulation of the E and F region electrodynamic coupling process that takes into account also its asymmetry about the magnetic equator arising from the finite magnetic declination angle. The results of the simulation show, in agreement with observations, that the occurrence time of the evening F region vertical drift prereversal peak and its seasonal variation at a station are controlled by the magnetic declination angle at that station, which determines the seasonal variation of the sunset times (and hence the Integrated Pedersen conductivity longitudinal gradient) at its magnetic conjugate E layers. The amplitude of the prereversal peak, on the other hand, undergoes the influence of the magnetic declination angle as well as of the thermospheric zonal wind component.

87 equador magnético

87 região F

87 condutividade

87 movimento de plasma

88 magnetic equator

88 F region

88 conductivity

88 plasma drift

91 FDB - 19980831

92 FDB - EGCF

EQUATORIAL F REGION VERTICAL PLASMA DRIFTS:
SEASONAL AND LONGITUDINAL ASYMMETRIES IN THE AMERICAN SECTOR

I. S. Batista, M. A. Abdu, and J. A. Bittencourt

Instituto de Pesquisas Espaciais, São José dos Campos, São Paulo, Brazil

Abstract. Longitudinal and seasonal asymmetries in the evening ionospheric F region plasma vertical drift (V_z) enhancements, between two longitudinally separated stations situated along the magnetic equator, in the American sector, are investigated under solar maximum conditions, based on results obtained from the analysis of ionosonde data for these stations. The two stations are Huancayo, Peru, and Fortaleza, Brazil, which have markedly different magnetic declination angles. The observed asymmetries are interpreted using a detailed numerical simulation of the E and F region electrodynamic coupling process that takes into account also its asymmetry about the magnetic equator arising from the finite magnetic declination angle. The results of the simulation show, in agreement with observations, that the occurrence time of the evening F region vertical drift prereversal peak and its seasonal variation at a station are controlled by the magnetic declination angle at that station, which determines the seasonal variation of the sunset times (and hence the integrated Pedersen conductivity longitudinal gradient) at its magnetic conjugate E layers. The amplitude of the prereversal peak, on the other hand, undergoes the influence of the magnetic declination angle as well as of the thermospheric zonal wind component.

1. Introduction

Ionospheric F region plasma vertical drifts have been extensively measured at Jicamarca Radar Observatory [Woodman, 1970; Balsley, 1973; Woodman et al., 1977; Fejer et al., 1979a], a magnetic equatorial station (12°S , 77°W ; magnetic dip 0.9°), and theoretically simulated by Heelis et al. [1974]. It is clear now that the F region vertical drift at Jicamarca (and its prereversal peak) shows large seasonal and solar cycle variation [Fejer et al., 1979a; Fejer, 1981] and, at times, the equatorial eastward electric field (that controls the upward drift) is also strongly influenced by high-latitude and magnetospheric phenomena driven ultimately by solar wind [Fejer et al., 1979b, 1983; Gonzales et al., 1979, 1983]. It is well known that the daytime equatorial F layer ionization moves upward due to the $E \times B$ drift arising from the eastward electric field induced by the E region dynamo. This electric field is reversed at night, causing also a reversal in the ionization drift velocity (V_z) to downward. Before its reversal, however, V_z undergoes a rapid enhancement, giving rise to a prereversal maximum (V_{zp}), believed to be caused by the buildup of the F region polarization elec-

tric field (namely, F region dynamo field produced by thermospheric winds) that arises from the decrease in the E layer conductivity following sunset [Rishbeth, 1971, 1977, 1981]. Therefore, it is reasonable to suppose that those F region polarization electric fields and the associated equatorial F region drifts are influenced by conductivity variations in the conjugate E layers (linked one to the other, via the equatorial ionospheric F region, by conducting magnetic field lines) and by the thermospheric zonal wind component.

In this work, F region vertical drifts derived from ionograms over Huancayo (12°S , 75°W ; magnetic dip 0.6°) are first compared with those simultaneously measured by the Jicamarca radar. It is seen that there is a good agreement between the results obtained from the two techniques only during the prereversal enhancement time and in its immediate vicinity, in agreement with the theoretical prediction of Bittencourt and Abdu [1981]. Ionosonde data are then used to derive F region vertical drifts around the prereversal peak for Huancayo, Peru, and Fortaleza, Brazil (3°S , 38°W ; magnetic dip -2°), two magnetic equatorial stations in the American zone, characterized by very different magnetic declination angles. In fact the magnetic declination of Huancayo is 3°E and that of Fortaleza is 21°W , which represents a global maximum in the longitudinal variation of that parameter. As was already pointed out by Abdu et al. [1981], the F region drift prereversal peak shows distinctly different seasonal behavior at these two locations. Through a numerical simulation of the electrodynamic coupling of the ionospheric E and F regions, that takes into account the asymmetry (namely the unequal Pedersen conductivities at the conjugate E layers) about the magnetic equator arising from finite magnetic declination angles, it is shown that those differences in the seasonal behavior can be explained on the basis of two major factors: the distinctly different magnetic declination angles at the two locations, and the seasonal variations of the thermospheric wind zonal component.

2. Experimental Results

The ionosonde data used in this work were obtained from the equatorial stations Fortaleza and Huancayo, whose locations are shown in Figure 1. Also shown in the same figure is the location of Jicamarca, whose radar vertical drift data will be compared with those derived from Huancayo ionograms, taken simultaneously with the radar measurements.

Since the number of incoherent scatter radars measuring ionospheric drifts at equatorial stations is very limited, it is always desirable to have other ways of inferring those parameters [Abdu et al., 1981]. Bittencourt and Abdu [1981]

Copyright 1986 by the American Geophysical Union.

Paper number 6A8488.
0148-0227/86/006A-8488\$05.00

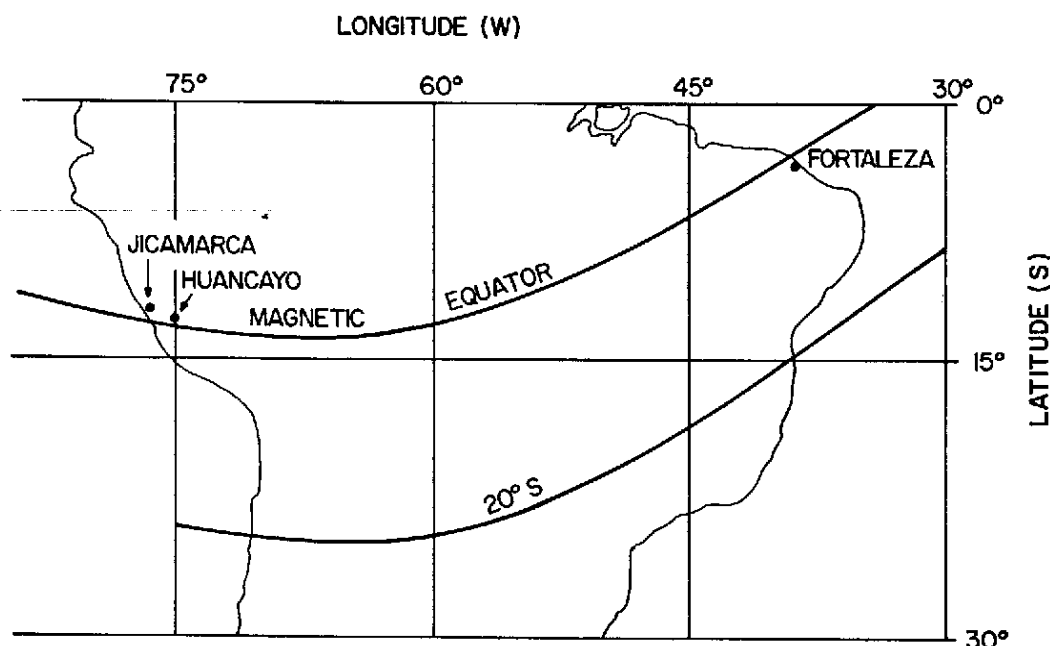


Fig. 1. Geographic and magnetic locations of Fortaleza, Huancayo, and Jicamarca included in the study.

showed that, at special time periods during sunset and evening hours, when the F layer height is above a threshold of 300 km, the apparent F layer vertical displacement velocity, inferred from ionosonde measurements, is the same as the vertical $E \times B$ plasma drift velocity, such as that determined from incoherent scatter radar measurements of the F region. For heights smaller than 300 km, the apparent vertical velocity starts to depart significantly from the vertical $E \times B$ drift velocity, owing to the increasing dominance of the recombination process at these lower heights. In Figure 2 we have presented a comparison of the vertical F layer velocities (V_z) measured by the Jicamarca radar with those simultaneously deduced as $\Delta(h'F)/\Delta t$ from Huancayo ionograms. Jicamarca vertical drift data were taken from Woodman [1970] and grouped to produce the mean diurnal variations representing equinoxes, winter (northern solstice), and summer (southern solstice) months, as means of 14, 20, and 7 days, respectively. F region virtual height ($h'F$) data were reduced each 15 minutes from Huancayo ionograms for exactly the same days when Jicamarca data were available.

We may notice in Figure 2 that the apparent vertical F layer drift, inferred from ionosonde measurements as $\Delta(h'F)/\Delta t$, is, as theoretically predicted [Bittencourt and Abdu, 1981], representative of the vertical $E \times B$ plasma drift velocity only around the times of prereversal vertical drift enhancements, when the layer is high, as can be verified from the $h'F$ values, also plotted in the same figure. Although the V_{zp} amplitudes deduced from ionograms do sometimes differ from those measured by incoherent scatter radar, the V_z prereversal peak occurrence times obtained by the two methods are indeed coincident, showing also similar seasonal trends. The V_z reversal times are found to be perfectly coincident during equinoxes and winter months; but not so perfectly

during the summer. Similar results were presented by Fejer [1981], who has made a comparison between the Jicamarca F region vertical drift reversal times and the reversal times inferred from Huancayo ionogram records during solar maximum. In view of the good agreement between the F region vertical drifts obtained by the Jicamarca radar and that obtained from Huancayo ionograms during the prereversal drift enhancements, we are using in the present work the Huancayo and Fortaleza ionogram records to infer the F region vertical drifts at sunset times, when the layer is high enough to supplant recombination effects.

In this work we have analyzed the data for the one-year period from October 1978 to September 1979, near the maximum of a solar cycle. During this period the F layer heights over Fortaleza and Huancayo, around sunset times, were well above 300 km, which gives better confidence in using ionosonde measurements to infer vertical drifts during their prereversal enhancements. In Figure 3 we have shown the vertical F layer velocity (V_z) monthly mean variation, around sunset, deduced as $\Delta(h'F)/\Delta t$ from Fortaleza and Huancayo ionograms for the period covered in the present study. The figure shows that in general the V_z amplitudes over Fortaleza are greater than over Huancayo for most of the time. We may notice further that the V_z evening prereversal maximum has highest amplitudes in the equinoxes and summer months (and lowest in winter) at both Fortaleza and Huancayo. However, the most outstanding feature in Figure 3 is the seasonal trend of the prereversal V_z peak time occurrence, as was already pointed out by Abdu et al. [1981]. Over Huancayo the V_z peak occurs earlier in winter and later in summer. Over Fortaleza, situated closer to the geographic equator, also in the southern hemisphere, some 37° eastward of Huancayo, the observed trend in Figure 3 is

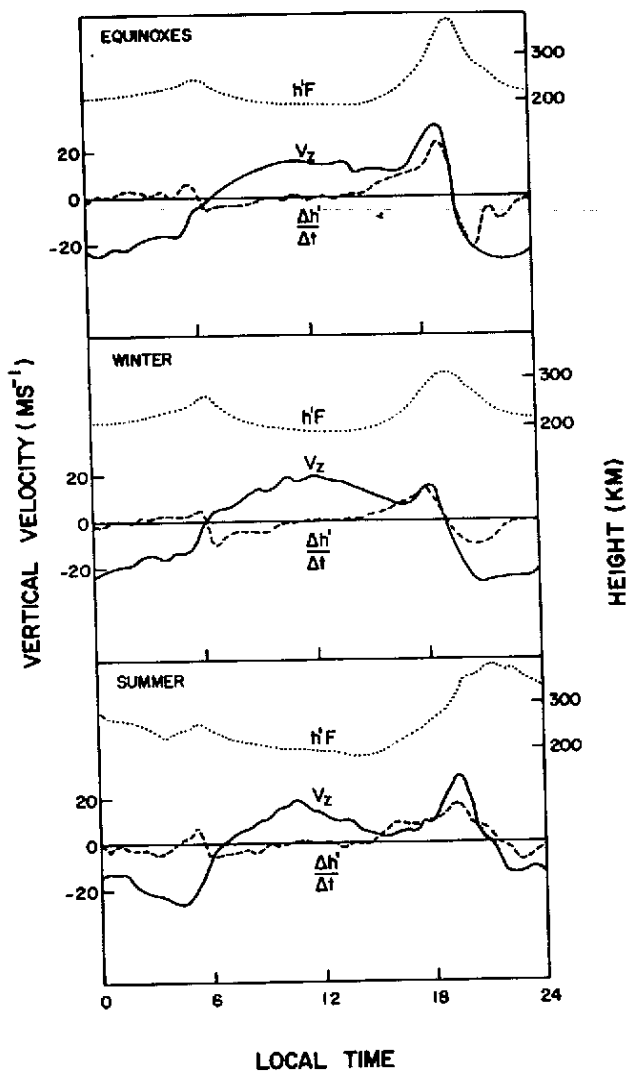


Fig. 2. Comparison between the mean F region vertical drift measured by Jicamarca radar (solid lines) and that simultaneously inferred using Huancayo ionograms (dashed lines) for equinoxes, summer, and winter. Also shown is the mean F layer minimum virtual height (dotted lines). Jicamarca vertical drift data were taken from Woodman [1970].

exactly opposite, namely, the V_z peak occurs earlier in summer and later in winter months. These different seasonal trends in V_{zp} have corresponding signatures in the seasonal spread F occurrence pattern as well, as pointed out by Abdu et al. [1981].

The equatorial F region vertical drift is controlled by the $E \times B$ drift arising from an east-west electric field. During daytime the source of this electric field is the E region field, which is mapped onto the F region by the highly conducting field lines (the polarization field that could be set up in the F region by thermospheric winds being short-circuited by the high E region conductivity). At night, however, the small E region conductivity causes a significant decrease in the short-circuiting effect, thus giving rise to the buildup of the F region

polarization electric fields generated by the zonal component of the thermospheric winds [Rishbeth, 1971, 1977]. Although this polarization field is mainly vertical during the night, there arise east-west components at sunset and sunrise times, when the electric current geometry is highly influenced by the rapid local time gradients in the E region integrated conductivity [Rishbeth, 1981; Heelis et al., 1974]. Thus, longitudinal (or local time) gradients in the E region conductivity (or in the electron density), which are present at the low-latitude magnetic conjugate E layers coupled to the equatorial F region by magnetic field lines, strongly influence the prereversal peak in the evening F region vertical drift. If, for example, only one of the

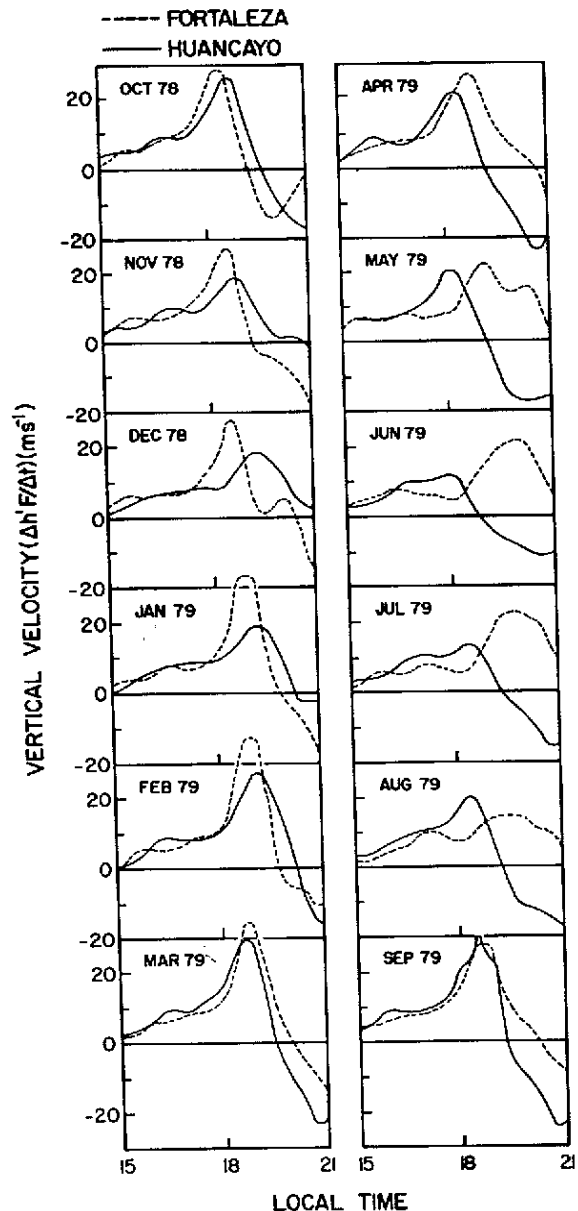


Fig. 3. F region vertical drift monthly means over Huancayo (solid lines) and Fortaleza (dashed lines) inferred as $\Delta(h'F)/\Delta t$ from ionograms around sunset time.

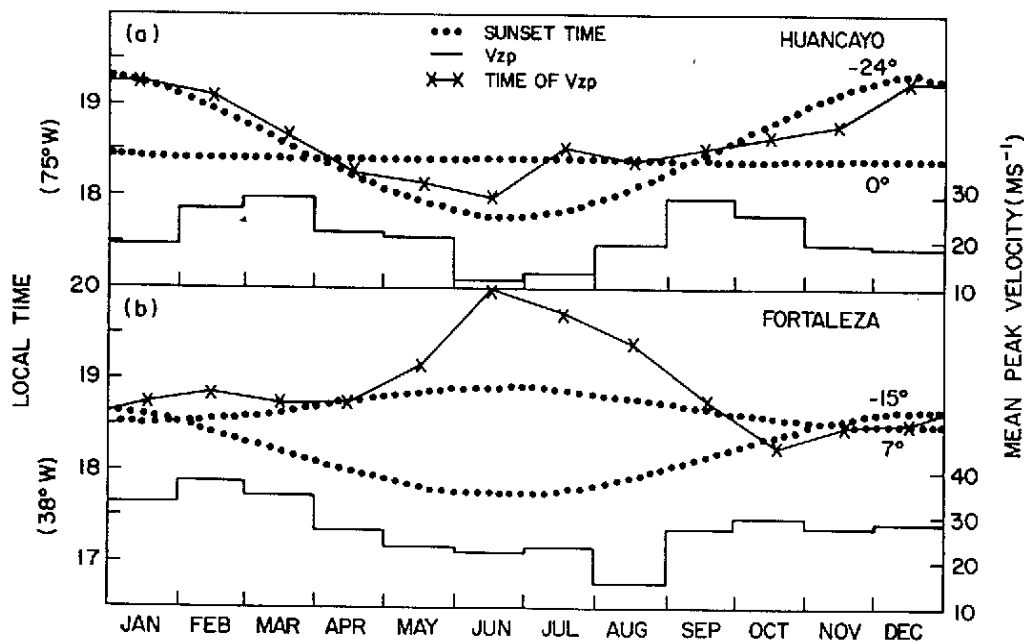


Fig. 4. Sunset time (dotted lines) calculated on the two magnetically conjugate E regions located north and south of (a) Huancayo and (b) Fortaleza. The numbers identifying each curve give the approximate geographical latitude of the E region under consideration. The histogramlike plots represent the V_{zp} amplitudes, and the crosses show the V_{zp} phase monthly mean.

low-latitude magnetic conjugate E layers is sunlit, still there will be a short-circuiting effect between the E and F regions. Thus the sunset times in the conjugate layers strongly influence the F layer drift prereversal enhancements. The sunset times in the conjugate E layers of Fortaleza show a seasonal variation distinctly different from that of Huancayo, due to the different magnetic declination angles of the two locations, which therefore give rise to the asymmetries in the longitudinal conductivity gradient between the respective conjugate E layers.

We have calculated the conjugate E layer sunset times corresponding to the Fortaleza and Huancayo locations (see Abdu et al. [1981] for details) for a one-year period, and the results are shown in Figure 4 as two dotted lines for each location, each dotted line representing one of the two magnetically conjugate E layers located north or south of the two equatorial stations. We can see that, for both the stations, there are two nodes when the E region sunset occurs simultaneously at both the magnetically conjugate locations, and this happens when the terminator is aligned with the magnetic meridian of the equatorial station. Over Huancayo (Figure 4a) these nodes are seen to occur during the equinoctial months because the magnetic declination angle over that station is very low (3°E). Over Fortaleza, which has a much higher magnetic declination angle (21°W), the nodes occur during the summer period (November, January-February). We can observe that the sunset duration (i.e., the time difference between the sunset times at the two conjugate E layers) over Huancayo has a maximum in December (53 min) and a secondary maximum in June (35 min). The maximum sunset duration over Fortaleza, which occurs in June (70

min), is greater than that over Huancayo, thus representing the slowest longitudinal variation in the E region conductivity.

In Figure 4, together with the sunset time at the conjugate E layers, we have shown also the V_{zp} amplitude (histogramlike plots) and phase (crosses) over Huancayo and Fortaleza for the one-year period under investigation (October 1978 to September 1979). We may note from the figure that the maxima in amplitudes are well correlated with the nodes in sunset times over both the stations when the terminator is aligned with the magnetic meridian and there is a sudden decrease in the E region conductivity. Over Fortaleza the amplitudes have a minimum during winter months, when the sunset duration shows a maximum. Abdu et al. [1981] have noted correlation among sunset duration, V_z peak width, and range spread F occurrences. It was noted, for example, that during the season where the sunset duration was short, the V_z peak had higher amplitude with shorter width, and the range spread F occurrence was high. Tsunoda [1985] has shown that the occurrence maxima in scintillation activity at a given longitude are coincident with times of the year when sunset is simultaneous at the conjugate E layers.

The relationship between the sunset duration and V_z peak amplitude does not, however, seem to be all that straightforward. For example, over Huancayo the amplitudes are greater during the summer than during the winter months, but the sunset durations in December are greater than in July, showing that there must be other factors, besides the longitudinal conductivity gradient, that have influence on the V_{zp} amplitudes. The V_{zp} phase shows a tendency to follow the sunset time at the magnetically conjugate E layer at which it occurs later. We observe some discrep-

ancies, however, the most outstanding being during winter months, over Fortaleza, where the maximum of V_{zp} occurs almost one hour later than the latest sunset time at the magnetically conjugate E layer.

The different magnetic field declination angles over Fortaleza and Huancayo cause the conjugate E region sunset times and their duration for the respective station to be significantly different and to occur with different seasonal trends. This is because, as explained earlier, the conjugate E regions are linked to the equatorial F region by magnetic field lines such that when the terminator is parallel to the field lines, the sunset occurs simultaneously at both the E regions (nodes in Figure 4), and no short-circuiting effect is operative later on, which therefore represents a sharp longitudinal conductivity gradient. On the other hand, if one of the E regions is sunlit while the other is dark, the short-circuiting effect is still effective and the conductivity has a slower longitudinal gradient. So, the magnetic field declination angle is an important factor in explaining the seasonal trends in the V_z prereversal peak parameters. Another important factor that must be taken into account to explain the V_{zp} seasonal variations is the thermospheric wind. The relative importance of these two factors in determining the observed amplitude and phase variations in V_{zp} will be investigated using a numerical simulation described in the following section.

3. The Vertical Drift Model

The electrodynamical coupling of the E and F regions is simulated by a theoretical model based on that developed by Heelis et al. [1974], and only a brief description of it will be given here.

In a spherical polar coordinate system (r, θ, ϕ) , where θ and ϕ coincide with magnetic colatitude and longitude, respectively, the E region electrostatic potential, $\psi(\theta, \phi)$, can be calculated from the equation

$$A \frac{\partial^2 \psi}{\partial \theta^2} + B \frac{\partial^2 \psi}{\partial \phi^2} + C \frac{\partial \psi}{\partial \theta} + D \frac{\partial \psi}{\partial \phi} = F \quad (1)$$

$0 \leq \theta \leq \pi/2$, $0 \leq \phi \leq 2\pi$, with the following boundary conditions:

$$\psi(0, \phi) = 0 \quad \left. \frac{\partial \psi(\theta, \phi)}{\partial \theta} \right|_{\theta = \pi/2} = 0$$

$$\psi(\theta, 0) = \psi(\theta, 2\pi)$$

and where

$$A = \frac{1}{r_E} \sin \theta \Sigma_{\theta\theta} \quad B = \frac{1}{r_E} \frac{\Sigma_{\phi\phi}}{\sin \theta}$$

$$C = \frac{1}{r_E} \left\{ \frac{\partial}{\partial \theta} (\sin \theta \Sigma_{\theta\theta}) - \frac{\partial}{\partial \phi} \Sigma_{\theta\phi} \right\}$$

$$D = \frac{1}{r_E} \left\{ \frac{\partial}{\partial \theta} \Sigma_{\theta\phi} + \frac{1}{\sin \theta} \frac{\partial}{\partial \phi} \Sigma_{\phi\phi} \right\}$$

$$F = r_E j_{\parallel} \sin \theta \sin I$$

$$+ \frac{\partial}{\partial \theta} \left\{ B \sin I \sin \theta \left(\Sigma_{\theta\phi} U_{\theta}^E - \Sigma_{\theta\theta} U_{\phi}^E \right) \right\}$$

$$+ \frac{\partial}{\partial \phi} \left\{ B \sin I \left(\Sigma_{\theta\phi} U_{\phi}^E + \Sigma_{\phi\phi} U_{\theta}^E \right) \right\}$$

and where B is the earth magnetic field intensity, I is the dip angle, r_E is the E region radius, $\Sigma_{\theta\theta}$, $\Sigma_{\theta\phi}$, and $\Sigma_{\phi\phi}$ are the layer conductivities, U_{θ}^E and U_{ϕ}^E are the zonal and meridional components of the E region tidal wind velocity, and j_{\parallel} is the field-aligned current flowing along a field line at the base of the F region.

If the E region electrostatic potential is known, the electric field in the F region can be calculated by mapping the E region electrostatic field at any point of a field line.

Assuming equivalence between longitude (ϕ) and local time (t) variations, the east-west component of the thermospheric neutral wind, $U(r, t)$, may be calculated from the following equation:

$$P \frac{\partial U}{\partial t} = \frac{\partial^2 U}{\partial r^2} + Q \frac{\partial U}{\partial r} + RU + S \quad (2)$$

$0 \leq t \leq T$, $r_0 \leq r \leq r_1$, with the following initial and boundary conditions:

$$U(r, 0) = U(r, T) \quad U(r_0, t) = 0$$

$$\left. \frac{\partial U(r, t)}{\partial r} \right|_{r=r_1} = 0$$

where

$$P = \frac{\rho}{\mu} \left(1 + \frac{U}{\Omega} \right)$$

$$Q = \frac{2}{r}$$

$$R = - \frac{1}{r^2 \sin^2 \theta} - \frac{\rho N v}{\mu n} \frac{1}{1 + (v/\omega)^2}$$

$$S = \frac{\rho N v}{\mu n} \frac{(v/\omega) E_{\phi} - E_n}{B[1 + (v/\omega)^2]} - \frac{1}{\mu r \sin \theta} \frac{\partial p}{\partial \phi}$$

where Ω is the rotational speed of the earth, ω is the ion gyrofrequency, v is the effective ion-neutral collision frequency, μ is the molecular viscosity coefficient, N is the ion concentration, n , ρ , and p are the concentration, density, and pressure, respectively, of the neutral atmosphere, and E_n and E_{ϕ} are the electric field components in the two directions perpendicular to the magnetic field line (in the coordinate system (n, s, ϕ) ; n is perpendicular to the magnetic field line and directed upward, s is parallel to the field line and directed

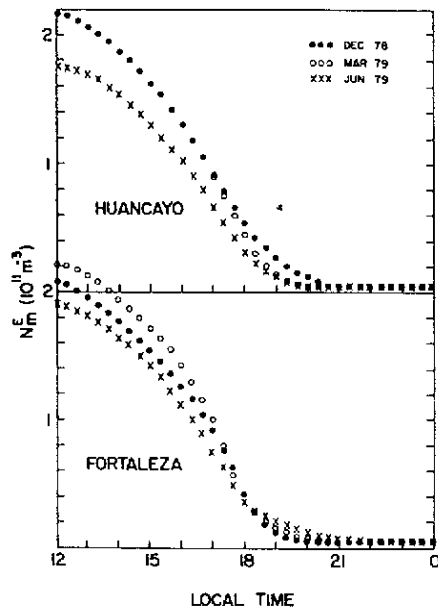


Fig. 5. Local time variation of the peak E region electron density used in the simulations for Huancayo and Fortaleza representing December 1978 (solid circles), March 1979 (open circles), and June 1979 (crosses).

toward the equator in the northern hemisphere, and ϕ is the magnetic longitude directed eastward).

The drift velocities of the ions in the F region (V_n and V_ϕ) and the normal current components (j_n and j_ϕ) can be calculated using the expressions

$$[1 + (v/\omega)^2] V_n = \frac{v}{\omega} U + \frac{v}{\omega} \frac{E_n}{B} + \frac{E_\phi}{B} \quad (3)$$

$$[1 + (v/\omega)^2] V_\phi = \left(\frac{v}{\omega}\right)^2 U + \frac{v}{\omega} \frac{E_\phi}{B} - \frac{E_n}{B}$$

$$j_n = Ne \frac{v}{\omega} (U - V_\phi) \quad (4)$$

$$j_\phi = Ne \frac{v}{\omega} V_n$$

and finally the field-aligned current flowing along a field line at the base of the F region can be obtained by solving the integration

$$j_{||} = \frac{(1 + 3 \cos^2 \theta)^{1/2}}{r^3} \cdot \int_{s_1}^{s_2} \frac{r^3}{(1 + 3 \cos^2 \theta)^{1/2}} \left[\frac{\partial j_n}{\partial n} + j_n \nabla \cdot \hat{n} \right] ds \quad (5)$$

where s_1 and s_2 are the points where the field line crosses the base of the F region and the magnetic equator, respectively.

The E and F region equations described above

are solved self-consistently. The coupling parameter between the E and F regions is the field-aligned current, $j_{||}$, at the base of the F region. Initially, this field-aligned current is assumed to be zero. Then, the E region electrostatic potential generated by a diurnal tidal wind is calculated by numerically solving equation (1) (which is an elliptic partial differential equation) using finite difference and successive overrelaxation [Young, 1971]. This electrostatic potential is used to find the E region polarization electric field which, mapped onto the F region via magnetic field lines, controls the plasma drifts and currents there. In the F region, the thermospheric zonal wind velocity is calculated by solving (2), which is a parabolic nonlinear partial differential equation. This equation is approximated by finite differences, leading to a tridiagonal system that is solved using the Crank-Nicholson method and the Gauss elimination algorithm [Potter, 1973]. The F region drifts and currents are then calculated using (3) and (4), and a new value of the field-aligned current is found by numerically integrating (5) along a field line. This new $j_{||}$ is used to start again the E region calculations, and the process continues until a steady state situation is reached.

The basic difference between Heelis et al.'s [1974] model and ours is that they have assumed that all parameters are symmetrical about the equator, while here we have assumed asymmetric conditions, owing to the very high value of the magnetic declination angle we are concerned about. To do this we have constructed different conductivity diurnal variation curves, representative of three seasons for the conjugate E layers corresponding to Huancayo and Fortaleza. Following Heelis et al. [1974], the conductivity model was supposed proportional to the peak E region electron density (N_m^E).

Figure 5 shows the diurnal variation of N_m^E for December 1978 (solid circles), March 1979 (open circles) and June 1979 (crosses), obtained as the mean of the variations at the two magnetically conjugate E regions situated along the same magnetic meridian, plotted separately for Huancayo and Fortaleza. These curves were based on the peak E region electron density values deduced from Huancayo and Fortaleza ionograms for the period under investigation. The E region electron density (and the conductivity) in each conjugate E region was supposed to reach a constant value at night, in a time determined by the sunset times given in Figure 4. The resultant N_m^E plots, shown in Figure 5, already take into account the asymmetry about the magnetic equator, due to the magnetic declination angle, because they represent a mean value between the two conjugate E layers. Although the N_m^E absolute values near sunset hours at a given location may not be very precise, their relative seasonal behaviors shown in Figure 5 are reasonably correct owing to the fact that they were based on the conjugate E region sunset times.

With the exception of the E and F region peak electron density and the atomic oxygen distribution, all the other atmospheric parameters were the same as described by Heelis et al. [1974]. The N_m^E values were obtained in the way described above, and the F region peak electron densities

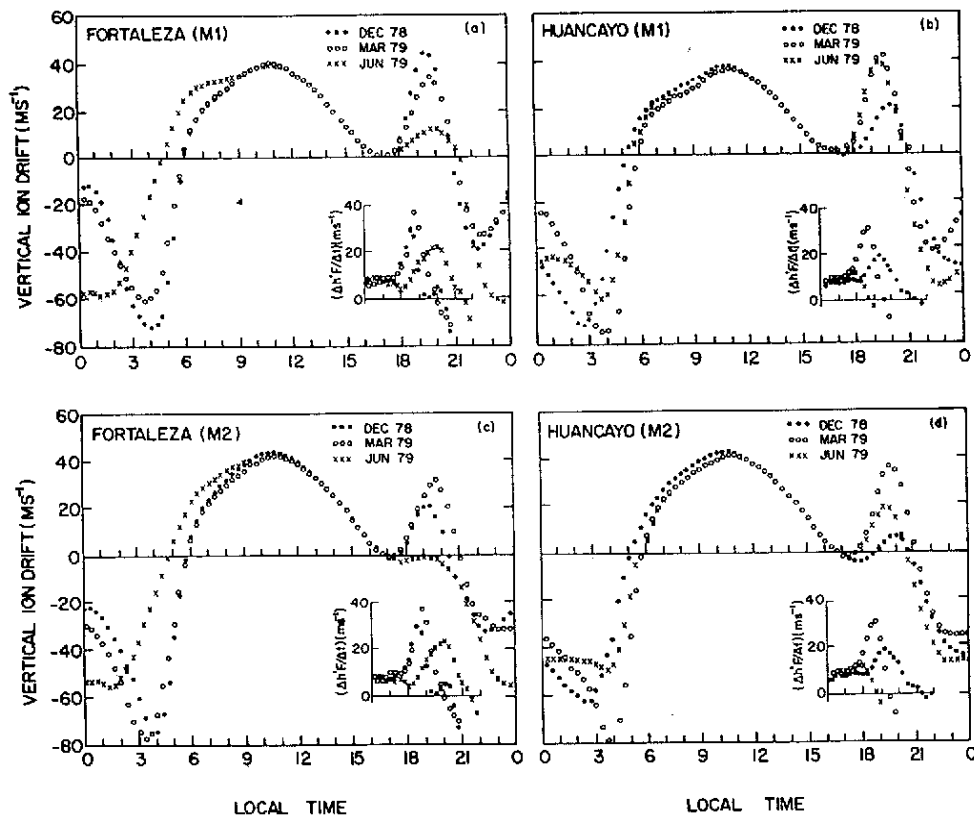


Fig. 6. Local time variation of the vertical ion velocity at 300 km above (a and c) Fortaleza and (b and d) Huancayo for December 1978 (solid circles), March 1979 (open circles), and June 1979 (crosses). Figures 6a and 6b were obtained using the M1 simulation, and Figures 6c and 6d using the M2 simulation. Also shown in the insets are the vertical ion velocity inferred from Huancayo and Fortaleza ionograms as $\Delta(h'F)/\Delta t$ during sunset time (the horizontal time scales of the calculated and inferred vertical ion drifts are the same).

were deduced from Huancayo and Fortaleza ionograms, for the period under consideration. We have considered two different atomic oxygen distribution models as follows. In the first simulation, here denoted by M1, we have used the same atomic oxygen distribution as given by Heelis et al. [1974]. Thus, the M1 simulation has assumed the same atomic oxygen distribution for the three seasons, irrespective of the geographic location under consideration. In the second simulation, here denoted by M2, we have used the neutral atmospheric parameters given by the Jacchia [1977] model. This procedure has given us the opportunity of investigating the influence of the neutral wind on the F region vertical drift prereversal peak, because the neutral atmosphere parameters that vary with season and location as per this model produce corresponding variations in neutral winds that are therefore representative of the respective seasons. Detailed discussions of the numerical simulation and atmospheric parameters used in the calculations are described by Batista [1986].

4. Results and Discussions

The equatorial F region vertical drifts were calculated using the numerical simulation technique as described above. The mean F region

vertical plasma drift diurnal variations at 300 km over the equator, calculated for both the M1 and M2 models, are shown in Figure 6, over Fortaleza and Huancayo, for December 1978, March 1979, and June 1979, representing the three seasons. Also in the same figure, the vertical plasma drifts inferred from Huancayo and Fortaleza ionograms as $\Delta(h'F)/\Delta t$ are shown for the same months as those used in the simulation. The mean behavior of the vertical drift diurnal variation shown in Figure 6 is in good agreement with the Jicamarca vertical drift measurements during sunspot maxima presented by Fejer et al. [1979a] and with that calculated by Heelis et al. [1974]. The drift is upward during the day, showing a maximum between 1000 LT and 1100 LT, and downward during the night, and it shows an evening prereversal enhancement.

In Figure 7 we have given emphasis to the comparison between observed and calculated vertical drifts. So, only the drifts during sunset hours for both Fortaleza and Huancayo were plotted. We can compare the simulated prereversal peak occurrence times with the ones inferred from Huancayo and Fortaleza ionograms that are shown in Figure 7 as $\Delta(h'F)/\Delta t$. It is observed that the prereversal maximum occurs earlier in December and later in June over Fortaleza. The M1 simulation gives the same relative

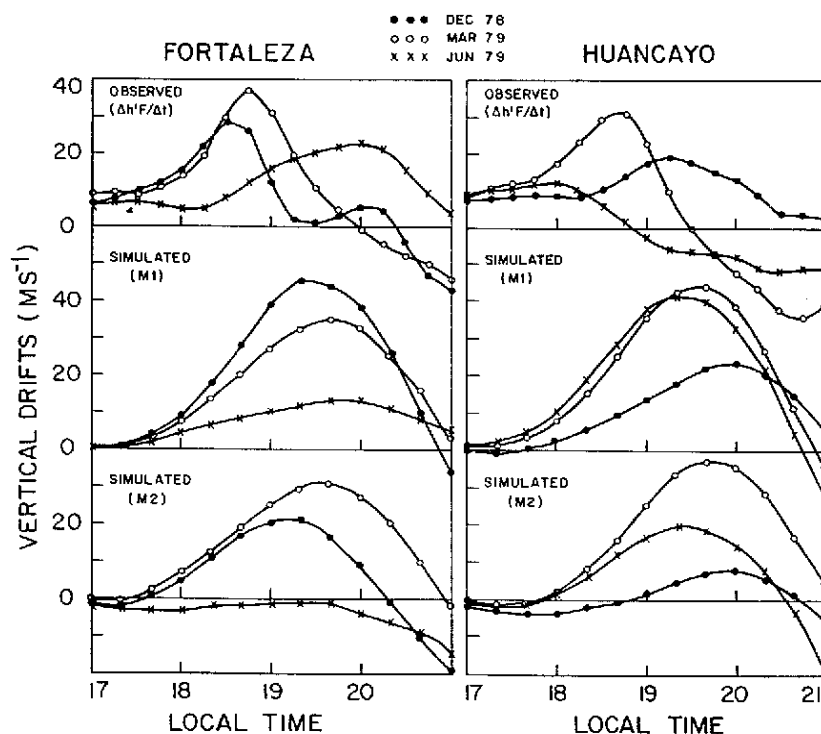


Fig. 7. Comparison between the vertical ion drifts inferred from ionograms as $\Delta(h'F)/\Delta t$ and simulated using the M1 and M2 models for Fortaleza and Huancayo.

behavior although it is only in June that the calculated and observed occurrence times of the prereversal peaks are coincident. In spite of the fact that the M2 simulation failed in producing a prereversal peak in June, over Fortaleza (the explanation for this will be given later), we can see that in this simulation the relative behavior of the prereversal maximum is maintained, that is, it occurs earlier in December and later in March. Over Huancayo the prereversal maximum occurs earlier in June and later in December, and this feature can be seen in both observed and simulated results (right part of Figure 7) although the calculated and observed occurrence times of the prereversal peaks are not coincident. It is important to note that the calculated prereversal peak occurrence time and its seasonal trend do not change with the M1 versus the M2 simulation.

The other aspect that can be analyzed is the V_z prereversal peak amplitude. We can see from Fortaleza data reproduced in Figure 6a, as $\Delta(h'F)/\Delta t$, that the highest V_{zp} amplitude occurs in March and the lowest one in June. Using the M1 simulation we can observe that the V_{zp} amplitude in December, over Fortaleza, is greater than in March, which does not agree with observations. Over Huancayo, on the other hand, we see that the M1 simulation leads to a result with similar amplitudes in March and June, and with the lowest value in December (Figure 6b), although the observations show the highest V_{zp} amplitude in March and the lowest in June.

The E and F region peak electron densities, N_m^E and N_m^F , are the only two parameters whose variations from one month to the other and from one station to the other are taken into account in

the M1 simulation. It was observed that the N_m^F variations have no significant influence on the vertical drift prereversal enhancements. So, the observed V_{zp} seasonal variations over Huancayo and Fortaleza are mainly due to the N_m^E (or integrated conductivity) variations. Therefore we can conclude that the different conductivities used in the simulation have influenced both the amplitude and the occurrence time of the vertical drift prereversal peak. In this way, from Figures 5 and 7 we can see that the later the conductivity gradient goes to zero (N_m^E reaches a constant value at night), the later the vertical drift prereversal peak occurs (June over Fortaleza and December over Huancayo). Regarding this aspect, the simulated results are in good agreement with observations. The influence of the conductivity longitudinal gradient on the V_{zp} amplitude can be summarized as follows. The V_{zp} amplitude is higher when the conductivity shows a faster longitudinal variation in the evening (December over Fortaleza and March over Huancayo) than when the conductivity longitudinal variation is slower (June over Fortaleza and December over Huancayo). The V_{zp} amplitude relative behavior simulated by the M1 model is not in agreement with the observations.

The M1 simulation indeed serves to demonstrate the influence on the F region vertical drift prereversal peak, due to the conductivity longitudinal profiles that were obtained taking into account the different magnetic declination angles over Huancayo and Fortaleza. In order to analyze the thermospheric wind effects on the F region vertical drifts, we carried out the M2 simulation, in which the atomic oxygen number densities were derived from Jacchia's [1977] model for the three

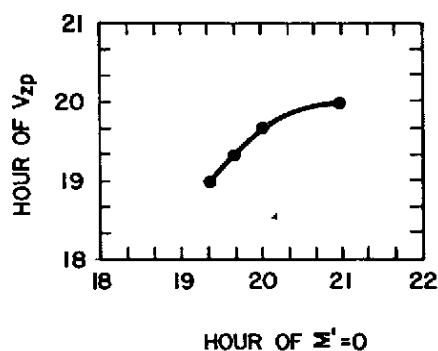


Fig. 8. Calculated F region vertical drift peak occurrence time (times of V_{zp}) versus the time when the conductivity longitudinal gradient (Σ') goes to zero.

months under consideration, over Fortaleza and Huancayo. The different atomic oxygen number densities ($n(0)$) obtained from the model give rise to different thermospheric winds that are representative for each station and season. The M2 simulation results are shown in Figure 6c and 6d for a 24-hour period, and in the lower part of Figure 7 during the sunset hours.

The F region vertical drift diurnal variations calculated using the M2 simulation for December 1978 and March and June 1979 over Fortaleza are shown in Figure 6c, and the seasonal behavior of the prereversal peak is shown separately in Figure 7. In this simulation the highest thermospheric winds over Fortaleza are obtained in March, with lower values in December and June. The calculated amplitude relative behavior of the F region vertical drift presents a significant modification when compared with the M1 simulation results. While in the M1 simulation, in which we have used the same $n(0)$ model in the three seasons, the highest V_{zp} amplitude had been obtained in December, in the M2 simulation the highest values are observed in March. On the other hand, the June V_{zp} amplitude was already low in the M1 simulation, and thus the lowest thermospheric wind used for June in the M2 simulation as well was insufficient to produce any significant amplitude for the V_z prereversal peak. Nevertheless the observed relative V_{zp} amplitude seasonal behavior (V_{zp} in March $> V_{zp}$ in December $> V_{zp}$ in June) has been better simulated by the M2 model than by the M1, although it seems that the thermospheric wind intensity of the M2 model is, in particular, underestimated for June. It should be pointed out that the V_{zp} occurrence times obtained by the M2 model in December and March are coincident with those obtained by the M1 model for the same months. This shows that moderate (or typical) variations in $n(0)$ or thermospheric wind intensity do not influence the V_{zp} occurrence time.

The F region vertical drift diurnal variations calculated using the M2 simulation for December 1978 and March and June 1979 over Huancayo are shown in Figure 6d, and the seasonal behavior of the prereversal peak is shown separately in Figure 7. As was already observed over Fortaleza, a lower $n(0)$ (or thermospheric wind) value has resulted in lower V_{zp} amplitudes in December and June, but we note it has not altered the V_{zp}

occurrence time. It seems that the thermospheric winds of the M2 model for Huancayo are underestimated in December and overestimated in June. These discrepancies over Huancayo could be attributed in part to its departure from the geographic equator (12°S).

The conductivity longitudinal gradient (Σ') effect on the F region vertical drift prereversal peak occurrence time is illustrated in Figure 8. The V_{zp} occurrence times were obtained using four different simulations having the conductivity longitudinal gradient going to zero at different times. We can see a positive correlation between the two variables. The later the Σ' goes to zero, the later V_{zp} occurs, although this relation is not linear. As was already discussed in connection with Figures 4 and 5, the time when $\Sigma' \rightarrow 0$ (or the time when N_m^E reaches its night value, here supposed constant) depends on the sunset times over the two magnetically conjugate E layers that are coupled to the equatorial F region by magnetic field lines. The sunset times at each conjugate E layer show a seasonal variation dependent on the magnetic declination angle. Therefore the equatorial station magnetic declination angle strongly influences the V_{zp} occurrence time seasonal behavior, as was already seen in the Fortaleza and Huancayo data (Figure 4).

5. Conclusions

It became clear from the previous discussions that it is possible to simulate the equatorial F region vertical drift prereversal behavior at a given location, conveniently choosing the conductivity models and the neutral atmosphere parameters. The V_{zp} occurrence time can be obtained by choosing appropriate conductivity longitudinal gradients, with $\Sigma' \rightarrow 0$ at a time that can be derived from Figure 8. This initial procedure will result in a V_{zp} amplitude that can be modified by using the appropriate neutral atmosphere parameters. From simulations for different test winds we have observed that a 30 percent decrease in the atomic oxygen density profile causes a 50 percent decrease in the V_z amplitudes near and at the local time of the prereversal peak. On the other hand, at local times further away from the prereversal peak, the corresponding V_z reduction is less than 20 percent, and during daytime hours a small increase (of about 5 percent) is observed in V_z with decreasing $n(0)$. Therefore, the observed seasonal V_{zp} behavior over Fortaleza and Huancayo can be explained on the basis of the magnetic declination angle influences on the conjugate E layer integrated Pedersen conductivity longitudinal gradients and of the thermospheric wind seasonal variations. The asymmetry about the magnetic equator, included in the simulation, was useful to show that the V_{zp} occurrence time is controlled by the longitudinal conductivity gradients at the conjugate E regions, through the magnetic declination angle, and that the V_{zp} amplitudes undergo the influence of both magnetic declination angle and thermospheric winds.

Acknowledgments. The Huancayo ionograms used in connection with this work were provided by the World Data Center A for Solar Terrestrial Physics. This work was partially supported by the "Fundo

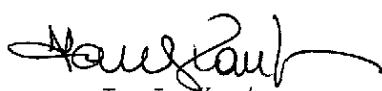
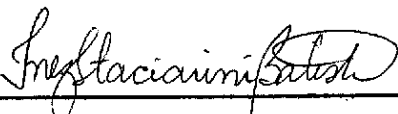
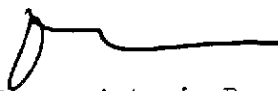
Nacional de Desenvolvimento Científico e Tecnológico" under contract FINEP 537/CT.

The Editor thanks H. Rishbeth and another referee for their assistance in evaluating this paper.

References

- Abdu, M. A., J. A. Bittencourt, and I. S. Batista, Magnetic declination control of the equatorial F region dynamo electric field development and spread F, *J. Geophys. Res.*, **86**, 11443, 1981.
- Balsley, B. B., Electric fields in the equatorial ionosphere: A review of techniques and measurements, *J. Atmos. Terr. Phys.*, **35**, 1035, 1973.
- Batista, I. S., *Dinamo da região F equatorial: Assimetrias sazonais e longitudinais no setor Americano*, Ph.D. thesis, Rep. INPE-3760-TDL/206, Inst. de Pesqui. Espaciais, São José dos Campos, S. P., Brazil, 1986.
- Bittencourt, J. A., and M. A. Abdu, A theoretical comparison between apparent and real vertical ionization drift velocities in the equatorial F region, *J. Geophys. Res.*, **86**, 2451, 1981.
- Fejer, B. G., The equatorial ionospheric electric field: A review, *J. Atmos. Terr. Phys.*, **43**, 377, 1981.
- Fejer, B. G., D. T. Farley, R. F. Woodman, and C. Calderon, Dependence of equatorial F region vertical drifts on season and solar cycle, *J. Geophys. Res.*, **84**, 5792, 1979a.
- Fejer, B. G., C. A. Gonzales, D. T. Farley, M. C. Kelley, and R. F. Woodman, Equatorial electric fields during magnetically disturbed conditions, 1, The effect of the interplanetary magnetic field, *J. Geophys. Res.*, **84**, 5797, 1979b.
- Fejer, B. G., M. F. Larsen, and D. T. Farley, Equatorial disturbance dynamo electric fields, *Geophys. Res. Lett.*, **10**, 537, 1983.
- Gonzales, C. A., M. C. Kelley, B. G. Fejer, J. F. Vickrey, and R. F. Woodman, Equatorial electric fields during magnetically disturbed conditions, 2, Implications of simultaneous auroral and equatorial measurements, *J. Geophys. Res.*, **84**, 5803, 1979.
- Gonzales, C. A., M. C. Kelley, R. A. Behnke, J. F. Vickrey, R. Wand, and J. Holt, On the latitudinal variation of the ionospheric electric field during magnetospheric disturbances, *J. Geophys. Res.*, **88**, 9135, 1983.
- Heelis, R. A., P. C. Kendall, R. J. Moffett, D. W. Windle, and H. Rishbeth, Electrical coupling of the E and F regions and its effect on F region drifts and winds, *Planet. Space Sci.*, **22**, 743, 1974.
- Jacchia, L. G., Thermospheric temperature, density, and compositions: New models, *Spec. Rep. 375*, Smithsonian Astrophys. Obs., Cambridge, Mass., 1977.
- Potter, D., *Computational Physics*, John Wiley, New York, 1973.
- Rishbeth, H., Polarization fields produced by winds in the equatorial F region, *Planet. Space Sci.*, **19**, 357, 1971.
- Rishbeth, H., Dynamics of equatorial F region, *J. Atmos. Terr. Phys.*, **39**, 1159, 1977.
- Rishbeth, H., The F region dynamo, *J. Atmos. Terr. Phys.*, **43**, 387, 1981.
- Tsunoda, R. T., Control of the seasonal and longitudinal occurrence of equatorial scintillations by the longitudinal gradient in integrated E region Pedersen conductivity, *J. Geophys. Res.*, **90**, 447, 1985.
- Woodman, R. F., Vertical drift velocities and east-west electric fields at the magnetic equator, *J. Geophys. Res.*, **75**, 6249, 1970.
- Woodman, R. F., R. G. Rastogi, and C. Calderon, Solar cycle effects on the electric fields in the equatorial ionosphere, *J. Geophys. Res.*, **82**, 5257, 1977.
- Young, D. M., *Iterative Solution of Large Linear Systems*, Academic, Orlando, Fla., 1971.
- I. S. Batista, M. A. Abdu, and J. A. Bittencourt, Instituto de Pesquisas Espaciais, Av. dos Astronautas, 1758, Caixa Postal 515, 12201 São José dos Campos, SP, Brazil.

(Received March 27, 1986;
revised June 26, 1986;
accepted June 30, 1986.)

1. Publication Nº INPE-3839-PRE/909	2. Version 3rd*	3. Date March, 1986	5. Distribution <input type="checkbox"/> Internal <input checked="" type="checkbox"/> External <input type="checkbox"/> Restricted
4. Origin DGA/DIO	Program IONO		
6. Key words - selected by the author(s) PREREVERSAL PEAK IONOSPHERIC PLASMA VERTICAL PLASMA DRIFTS E AND F REGIONS ELECTRODYNAMICAL COUPLING			
7. U.D.C.: 523.4-8			
8. Title EQUATORIAL F REGION VERTICAL PLASMA DRIFTS: SEASONAL AND LONGITUDINAL ASYMMETRIES IN THE AMERICAN SECTOR		10. Nº of pages: 25	
		11. Last page: 24	
9. Authorship I.S. Batista M.A. Abdu J.A. Bittencourt		12. Revised by  I. J. Kantor	
Responsible author 		13. Authorized by  Marco Antonio Raupp Director General	
14. Abstract/Notes Longitudinal and seasonal asymmetries in the evening ionospheric F region plasma vertical drift (V_z) enhancements, between two longitudinally separated stations situated along the magnetic equator, in the American sector, are investigated under solar maximum conditions, based on results obtained from the analysis of ionosonde data for these stations. The two stations are Huancayo, Peru, and Fortaleza, Brazil, which have markedly different magnetic declination angles. The observed asymmetries are interpreted using a detailed numerical simulation of the E and F region electrodynamic coupling process that takes into account also its asymmetry about the magnetic equator arising from the finite magnetic declination angle. The results of the simulation show, in agreement with observations, that the occurrence time of the evening F region vertical drift prereversal peak and its seasonal variation at a station are controlled by the magnetic declination angle at that station, which determines the seasonal variation of the sunset times (and hence the integrated Pedersen conductivity longitudinal gradient) at its magnetic conjugate E layers. The amplitude of the prereversal peak, on the other hand, undergoes the influence of the magnetic declination angle as well as of the thermospheric zonal wind component.			
15. Remarks This work was partially supported by the "Fundo Nacional de Desenvolvimento Científico e Tecnológico" under contract FINEP-537/CT. This work is being submitted to Journal of Geophysical Research. *Revised work in September, 1986.			

(1)

EQUATORIAL F REGION VERTICAL PLASMA DRIFTS:
SEASONAL AND LONGITUDINAL ASYMMETRIES IN THE AMERICAN SECTOR

I. S. Batista, M. A. Abdu, and J. A. Bittencourt

Instituto de Pesquisas Espaciais, São José dos Campos, São Paulo, Brazil

Abstract. Longitudinal and seasonal asymmetries in the evening ionospheric F region plasma vertical drift (V_z) enhancements, between two longitudinally separated stations situated along the magnetic equator, in the American sector, are investigated under solar maximum conditions, based on results obtained from the analysis of ionosonde data for these stations. The two stations are Huancayo, Peru, and Fortaleza, Brazil, which have markedly different magnetic declination angles. The observed asymmetries are interpreted using a detailed numerical simulation of the E and F region electrodynamic coupling process that takes into account also its asymmetry about the magnetic equator arising from the finite magnetic declination angle. The results of the simulation show, in agreement with observations, that the occurrence time of the evening F region vertical drift prereversal peak and its seasonal variation at a station are controlled by the magnetic declination angle at that station, which determines the seasonal variation of the sunset times (and hence the integrated Pedersen conductivity longitudinal gradient) at its magnetic conjugate E layers. The amplitude of the prereversal peak, on the other hand, undergoes the influence of the magnetic declination angle as well as of the thermospheric zonal wind component.

1. Introduction

Ionospheric F region plasma vertical drifts have been extensively measured at Jicamarca Radar Observatory [Woodman, 1970; Balsley, 1973, Woodman et al., 1977; Fejer et al., 1979a], a magnetic equatorial station (12°S , 77°W ; magnetic dip 0.9°), and theoretically simulated by Heelis et al. [1974]. It is clear now that the F region vertical drift at Jicamarca (and its prereversal peak) shows large seasonal and solar cycle variation [Fejer et al., 1979a; Fejer, 1981] and, at times, the equatorial eastward electric field (that controls the upward drift) is also strongly influenced by high-latitude and magnetospheric phenomena driven ultimately by solar wind [Fejer et al., 1979b, 1983; Gonzales et al., 1979, 1983]. It is well known that the daytime equatorial F layer ionization moves upward due to the $\mathbf{E} \times \mathbf{B}$ drift arising from the eastward electric field induced by the E region dynamo. This electric field is reversed at night, causing also a

reversal in the ionization drift velocity (V_z) to downward. Before its reversal, however, V_z undergoes a rapid enhancement, giving rise to a prereversal maximum (V_{zp}), believed to be caused by the buildup of the F region polarization electric field (namely, F region dynamo field produced by thermospheric winds) that arises from the decrease in the E layer conductivity following sunset [Rishbeth, 1971, 1977, 1981]. Therefore, it is reasonable to suppose that those F region polarization electric fields and the associated equatorial F region drifts are influenced by conductivity variations in the conjugate E layers (linked one to the other, via the equatorial ionospheric F region, by conducting magnetic field lines) and by the thermospheric zonal wind component.

In this work, F region vertical drifts derived from ionograms over Huancayo (12°S , 75°W ; magnetic dip 0.6°) are first compared with those simultaneously measured by the Jicamarca radar. It is seen that there is a good agreement between the results obtained from the two techniques only during the prereversal enhancement time and in its immediate vicinity, in agreement with the theoretical prediction of Bittencourt and Abdu [1981]. Ionosonde data are then used to derive F region vertical drifts around the prereversal peak for Huancayo, Peru, and Fortaleza, Brazil (3°S , 38°W ; magnetic dip -2°), two magnetic equatorial stations in the American zone, characterized by very different magnetic declination angles. In fact the magnetic declination of Huancayo is 3°E and that of Fortaleza is 21°W , which represents a global maximum in the longitudinal variation of that parameter. As was already pointed out by Abdu et al. [1981], the F region drift prereversal peak shows distinctly different seasonal behavior at these two locations. Through a numerical simulation of the electrodynamical coupling of the ionospheric E and F regions, that takes into account the asymmetry (namely the unequal Pedersen conductivities at the conjugate E layers) about the magnetic equator arising from finite magnetic declination angles, it is shown that those differences in the seasonal behavior can be explained on the basis of two major factors: the distinctly different magnetic declination angles at the two locations, and the seasonal variations of the thermospheric wind zonal component.

2. Experimental Results

The ionosonde data used in this work were obtained from the equatorial stations Fortaleza and Huancayo, whose locations are shown in Figure 1. Also shown in the same figure is the location of Jicamarca, whose radar vertical drift data

will be compared with those derived from Huancayo ionograms, taken simultaneously with the radar measurements.

Since the number of incoherent scatter radars measuring ionospheric drifts at equatorial stations is very limited, it is always desirable to have other ways of inferring those parameters [Abdu et al., 1981]. Bittencourt and Abdu [1981] showed that, at special time periods during sunset and evening hours, when the F layer height is above a threshold of 300 km, the apparent F layer vertical displacement velocity, inferred from ionosonde measurements, is the same as the vertical ExB plasma drift velocity, such as that determined from incoherent scatter radar measurements of the F region. For heights smaller than 300 km, the apparent vertical velocity starts to depart significantly from the vertical ExB drift velocity, owing to the increasing dominance of the recombination process at these lower heights. In Figure 2 we have presented a comparison of the vertical F layer velocities (V_z) measured by the Jicamarca radar with those simultaneously deduced as $\Delta(h'F)/\Delta t$ from Huancayo ionograms. Jicamarca vertical drift data were taken from Woodman [1970] and grouped to produce the mean diurnal variations representing equinoxes, winter (northern solstice), and summer (southern solstice) months, as means of 14, 20, and 7 days, respectively. F region virtual height ($h'F$) data were reduced each 15 minutes from Huancayo ionograms for exactly the same days when Jicamarca data were available.

We may notice in Figure 2 that the apparent vertical F layer drift, inferred from ionosonde measurements as $\Delta(h'F)/\Delta t$, is, as theoretically predicted [Bittencourt and Abdu, 1981], representative of the vertical ExB plasma drift velocity only around the times of prereversal vertical drift enhancements; when the layer is high, as can be verified from the $h'F$ values, also plotted in the same figure. Although the V_{zp} amplitudes deduced from ionograms do sometimes differ from those measured by incoherent scatter radar, the V_z prereversal peak occurrence times obtained by the two methods are indeed coincident, showing also similar seasonal trends. The V_z reversal times are found to be perfectly coincident during equinoxes and winter months, but not so perfectly during the summer. Similar results were presented by Fejer [1981], who has made a comparison between the Jicamarca F region vertical drift reversal times and the reversal times inferred from Huancayo ionogram records during solar maximum. In view of the good agreement between the F region vertical drifts obtained by the Jicamarca radar and that obtained from Huancayo ionograms during the prereversal drift enhancements, we are using in the present work the

Fig. 2

Huancayo and Fortaleza ionogram records to infer the F region vertical drifts at sunset times, when the layer is high enough to supplant recombination effects.

In this work we have analyzed the data for the one-year period from October 1978 to September 1979, near the maximum of a solar cycle. During this period the F layer heights over Fortaleza and Huancayo, around sunset times, were well above 300 km, which gives better confidence in using ionosonde measurements to infer vertical drifts during their prereversal enhancements. In Figure 3 we have shown the vertical F layer velocity (V_z) monthly mean variation, around sunset, deduced as $\Delta(h'F)/\Delta t$ from Fortaleza and Huancayo ionograms for the period covered in the present study. The figure shows that in general the V_z amplitudes over Fortaleza are greater than over Huancayo for most of the time. We may notice further that the V_z evening prereversal maximum has highest amplitudes in the equinoxes and summer months (and lowest in winter) at both Fortaleza and Huancayo. However, the most outstanding feature in Figure 3 is the seasonal trend of the prereversal V_z peak time occurrence, as was already pointed out by Abdu et al. [1981]. Over Huancayo the V_z peak occurs earlier in winter and later in summer. Over Fortaleza, situated closer to the geographic equator, also in the southern hemisphere, some 37° eastward of Huancayo, the observed trend in Figure 3 is exactly opposite, namely, the V_z peak occurs earlier in summer and later in winter months. These different seasonal trends in V_{zp} have corresponding signatures in the seasonal spread F occurrence pattern as well, as pointed out by Abdu et al. [1981].

The equatorial F region vertical drift is controlled by the $E \times B$ drift arising from an east-west electric field. During daytime the source of this electric field is the E region field, which is mapped onto the F region by the highly conducting field lines (the polarization field that could be set up in the F region by thermospheric winds being short-circuited by the high E region conductivity). At night, however, the small E region conductivity causes a significant decrease in the short-circuiting effect, thus giving rise to the buildup of the F region polarization electric fields generated by the zonal component of the thermospheric winds [Rishbeth, 1971, 1977]. Although this polarization field is mainly vertical during the night, there arise east-west components at sunset and sunrise times, when the electric current geometry is highly influenced by the rapid local time gradients in the E region integrated conductivity [Rishbeth, 1981; Heelis et al., 1974]. Thus, longitudinal (or local time) gradients in the E

Fig. 3

region conductivity (or in the electron density), which are present at the low-latitude magnetic conjugate E layers coupled to the equatorial F region by magnetic field lines, strongly influence the prereversal peak in the evening F region vertical drift. If, for example, only one of the low-latitude magnetic conjugate E layers is sunlit, still there will be a short-circuiting effect between the E and F regions. Thus the sunset times in the conjugate layers strongly influence the F layer drift prereversal enhancements. The sunset times in the conjugate E layers of Fortaleza show a seasonal variation distinctly different from that of Huancayo, due to the different magnetic declination angles of the two locations, which therefore give rise to the asymmetries in the longitudinal conductivity gradient between the respective conjugate E layers.

We have calculated the conjugate E layer sunset times corresponding to the Fortaleza and Huancayo locations (see Abdu et al. [1981] for details) for a one-year period, and the results are shown in Figure 4 as two dotted lines for each location, each dotted line representing one of the two magnetically conjugate E layers located north or south of the two equatorial stations. We can see that, for both the stations, there are two nodes when the E region sunset occurs simultaneously at both the magnetically conjugate locations, and this happens when the terminator is aligned with the magnetic meridian of the equatorial station. Over Huancayo (Figure 4a) these nodes are seen to occur during the equinoctial months because the magnetic declination angle over that station is very low (3°E). Over Fortaleza, which has a much higher magnetic declination angle (21°W), the nodes occur during the summer period (November, January-February). We can observe that the sunset duration (i.e., the time difference between the sunset times at the two conjugate E layers) over Huancayo has a maximum in December (53 min) and a secondary maximum in June (35 min). The maximum sunset duration over Fortaleza, which occurs in June (70 min), is greater than that over Huancayo, thus representing the slowest longitudinal variation in the E region conductivity.

In Figure 4, together with the sunset time at the conjugate E layers, we have shown also the V_{zp} amplitude (histogramlike plots) and phase (crosses) over Huancayo and Fortaleza for the one-year period under investigation (October 1978 to September 1979). We may note from the figure that the maxima in amplitudes are well correlated with the nodes in sunset times over both the stations when the terminator is aligned with the magnetic meridian and there is a sudden decrease in the E region conductivity. Over

6

Fortaleza the amplitudes have a minimum during winter months, when the sunset duration shows a maximum. Abdu et al. [1981] have noted correlation among sunset duration, V_z peak width, and range spread F occurrences. It was noted, for example, that during the season where the sunset duration was short, the V_z peak had higher amplitude with shorter width, and the range spread F occurrence was high. Tsunoda [1985] has shown that the occurrence maxima in scintillation activity at a given longitude are coincident with times of the year when sunset is simultaneous at the conjugate E layers.

The relationship between the sunset duration and V_z peak amplitude does not, however, seem to be all that straightforward. For example, over Huancayo the amplitudes are greater during the summer than during the winter months, but the sunset durations in December are greater than in July, showing that there must be other factors, besides the longitudinal conductivity gradient, that have influence on the V_{zp} amplitudes. The V_{zp} phase shows a tendency to follow the sunset time at the magnetically conjugate E layer at which it occurs later. We observe some discrepancies, however, the most outstanding being during winter months, over Fortaleza, where the maximum of V_{zp} occurs almost one hour later than the latest sunset time at the magnetically conjugate E layer.

The different magnetic field declination angles over Fortaleza and Huancayo cause the conjugate E region sunset times and their duration for the respective station to be significantly different and to occur with different seasonal trends. This is because, as explained earlier, the conjugate E regions are linked to the equatorial F region by magnetic field lines such that when the terminator is parallel to the field lines, the sunset occurs simultaneously at both the E regions (nodes in Figure 4), and no short-circuiting effect is operative later on, which therefore represents a sharp longitudinal conductivity gradient. On the other hand, if one of the E regions is sunlit while the other is dark, the short-circuiting effect is still effective and the conductivity has a slower longitudinal gradient. So, the magnetic field declination angle is an important factor in explaining the seasonal trends in the V_z prereversal peak parameters. Another important factor that must be taken into account to explain the V_{zp} seasonal variations is the thermospheric wind. The relative importance of these two factors in determining the observed amplitude and phase variations in V_{zp} will be investigated using a numerical simulation described in the following section.

3. The Vertical Drift Model

The electrodynamical coupling of the E and F regions is simulated by a theoretical model based on that developed by Heelis et al. [1974], and only a brief description of it will be given here.

In a spherical polar coordinate system (r, θ, ϕ) , where θ and ϕ coincide with magnetic colatitude and longitude, respectively, the E region electrostatic potential, $\psi(\theta, \phi)$, can be calculated from the equation

$$A \frac{\partial^2 \psi}{\partial \theta^2} + B \frac{\partial^2 \psi}{\partial \phi^2} + C \frac{\partial \psi}{\partial \theta} + D \frac{\partial \psi}{\partial \phi} = F \quad (1)$$

$0 \leq \theta \leq \pi/2$, $0 \leq \phi \leq 2\pi$, with the following boundary conditions:

$$\psi(0, \phi) = 0 \quad \left. \frac{\partial \psi(\theta, \phi)}{\partial \theta} \right|_{\theta = \pi/2} = 0$$

$$\psi(\theta, 0) = \psi(\theta, 2\pi)$$

and where

$$A = \frac{1}{r_E} \sin \theta \Sigma_{\theta\theta} \quad B = \frac{1}{r_E} \frac{\Sigma_{\phi\phi}}{\sin \theta}$$

$$C = \frac{1}{r_E} \left\{ \frac{\partial}{\partial \theta} (\sin \theta \Sigma_{\theta\theta}) - \frac{\partial}{\partial \phi} \Sigma_{\theta\phi} \right\}$$

$$D = \frac{1}{r_E} \left\{ \frac{\partial}{\partial \theta} \Sigma_{\theta\phi} + \frac{1}{\sin \theta} \frac{\partial}{\partial \phi} \Sigma_{\phi\phi} \right\}$$

$$F = r_E j_{||} \sin \theta \sin I$$

$$+ \frac{\partial}{\partial \theta} \left\{ B \sin I \sin \theta \left(\Sigma_{\theta\phi} U_{\theta}^E - \Sigma_{\theta\theta} U_{\phi}^E \right) \right\}$$

$$+ \frac{\partial}{\partial \phi} \left\{ B \sin I \left(\Sigma_{\theta\phi} U_{\phi}^E + \Sigma_{\phi\phi} U_{\theta}^E \right) \right\}$$

and where B is the earth magnetic field intensity, I is the dip angle, r_E is the E region radius, $\Sigma_{\theta\theta}$, $\Sigma_{\theta\phi}$, and $\Sigma_{\phi\phi}$ are the layer conductivities, U_{θ}^E and U_{ϕ}^E are the zonal and meridional components of the E region tidal wind velocity, and $j_{||}$ is the field-aligned current flowing along a field line at the base of the F region.

If the E region electrostatic potential is known, the electric field in the F region can be calculated by mapping the E region electrostatic field at any point of a field line.

Assuming equivalence between longitude (ϕ) and local time (t) variations, the east-west component of the thermospheric neutral wind, $U(r,t)$, may be calculated from the following equation:

$$P \frac{\partial U}{\partial t} = \frac{\partial^2 U}{\partial r^2} + Q \frac{\partial U}{\partial r} + RU + S \quad (2)$$

$0 \leq t \leq T$, $r_0 \leq r \leq r_1$, with the following initial and boundary conditions:

$$U(r,0) = U(r,T) \quad U(r_0,t) = 0$$

$$\left. \frac{\partial U(r,t)}{\partial r} \right|_{r=r_1} = 0$$

where

$$P = \frac{\rho}{\mu} \left(1 + \frac{U}{\Omega} \right)$$

$$Q = \frac{2}{r}$$

$$R = - \frac{1}{r^2 \sin^2 \theta} - \frac{\rho N \nu}{\mu n} \frac{1}{1 + (\nu/\omega)^2}$$

$$S = \frac{\rho N \nu}{\mu n} \frac{(\nu/\omega) E_\phi - E_n}{B[1 + (\nu/\omega)^2]} - \frac{1}{\mu r \sin \theta} \frac{\partial p}{\partial \phi}$$

where Ω is the rotational speed of the earth, ω is the ion gyrofrequency, ν is the effective ion-neutral collision frequency, μ is the molecular viscosity coefficient, N is the ion concentration, n , ρ , and p are the concentration, density, and pressure, respectively, of the neutral atmosphere, and E_n and E_ϕ are the electric field components in the two directions perpendicular to the magnetic field line (in the coordinate system (n, s, ϕ) ; n is perpendicular to the magnetic field line and directed upward, s is parallel to the field line and directed toward the equator in the northern hemisphere, and ϕ is the magnetic longitude directed eastward).

The drift velocities of the ions in the F region (V_n and V_ϕ) and the normal current components (j_n and j_ϕ) can be calculated using the expressions

$$\begin{aligned} [1 + (\nu/\omega)^2] V_n &= \frac{\nu}{\omega} U + \frac{\nu}{\omega} \frac{E_n}{B} + \frac{E_\phi}{B} \\ [1 + (\nu/\omega)^2] V_\phi &= \left(\frac{\nu}{\omega}\right)^2 U + \frac{\nu}{\omega} \frac{E_\phi}{B} - \frac{E_n}{B} \end{aligned} \quad (3)$$

$$j_n = Ne \frac{\nu}{\omega} (U - V_\phi) \quad (4)$$

$$j_\phi = Ne \frac{\nu}{\omega} V_n$$

and finally the field-aligned current flowing along a field line at the base of the F region can be obtained by solving the integration

$$j_n = \frac{(1 + 3 \cos^2 \theta)^{1/2}}{r^3} \int_{s_1}^{s_2} \frac{r^3}{(1 + 3 \cos^2 \theta)^{1/2}} \left\{ \frac{\partial j_n}{\partial n} + j_n \nabla \cdot \hat{n} \right\} ds \quad (5)$$

where s_1 and s_2 are the points where the field line crosses the base of the F region and the magnetic equator, respectively.

The E and F region equations described above are solved self-consistently. The coupling parameter between the E and F regions is the field-aligned current, j_n , at the base of the F region. Initially, this field-aligned current is assumed to be zero. Then, the E region electrostatic potential generated by a diurnal tidal wind is calculated by numerically solving equation (1) (which is an elliptic partial differential equation) using finite difference and successive overrelaxation [Young, 1971]. This electrostatic potential is used to find the E region polarization electric field which, mapped onto the F region via magnetic field lines, controls the plasma drifts and currents there. In the F region, the thermospheric zonal wind velocity is calculated by solving (2), which is a parabolic nonlinear partial differential equation. This equation is approximated by finite differences, leading to a tridiagonal system that is solved using the Crank-Nicholson method and the Gauss elimination algorithm [Potter, 1973].

The F region drifts and currents are then calculated using (3) and (4), and a new value of the field-aligned current is found by numerically integrating (5) along a field line. This new j_{\parallel} is used to start again the E region calculations, and the process continues until a steady state situation is reached.

The basic difference between Heelis et al.'s [1974] model and ours is that they have assumed that all parameters are symmetrical about the equator, while here we have assumed asymmetric conditions, owing to the very high value of the magnetic declination angle we are concerned about. To do this we have constructed different conductivity diurnal variation curves, representative of three seasons for the conjugate E layers corresponding to Huancayo and Fortaleza. Following Heelis et al. [1974], the conductivity model was supposed proportional to the peak E region electron density (N_m^E).

Figure 5 shows the diurnal variation of N_m^E for December 1978 (solid circles), March 1979 (open circles) and June 1979 (crosses), obtained as the mean of the variations at the two magnetically conjugate E regions situated along the same magnetic meridian, plotted separately for Huancayo and Fortaleza. These curves were based on the peak E region electron density values deduced from Huancayo and Fortaleza ionograms for the period under investigation. The E region electron density (and the conductivity) in each conjugate E region was supposed to reach a constant value at night, in a time determined by the sunset times given in Figure 4. The resultant N_m^E plots, shown in Figure 5, already take into account the asymmetry about the magnetic equator, due to the magnetic declination angle, because they represent a mean value between the two conjugate E layers. Although the N_m^E absolute values near sunset hours at a given location may not be very precise, their relative seasonal behaviors shown in Figure 5 are reasonably correct owing to the fact that they were based on the conjugate E region sunset times.

With the exception of the E and F region peak electron density and the atomic oxygen distribution, all the other atmospheric parameters were the same as described by Heelis et al. [1974]. The N_m^E values were obtained in the way described above, and the F region peak electron densities were deduced from Huancayo and Fortaleza ionograms, for the period under consideration. We have considered two different atomic oxygen distribution models as follows. In the first simulation, here denoted by M1, we have used the same atomic oxygen distribution as given by Heelis et al. [1974]. Thus, the M1 simulation has assumed the same atomic oxygen distribution for the three seasons, irrespective of the

geographic location under consideration. In the second simulation, here denoted by M2, we have used the neutral atmospheric parameters given by the Jacchia [1977] model. This procedure has given us the opportunity of investigating the influence of the neutral wind on the F region vertical drift prereversal peak, because the neutral atmosphere parameters that vary with season and location as per this model produce corresponding variations in neutral winds that are therefore representative of the respective seasons. Detailed discussions of the numerical simulation and atmospheric parameters used in the calculations are described by Batista [1986].

4. Results and Discussions

The equatorial F region vertical drifts were calculated using the numerical simulation technique as described above. The mean F region vertical plasma drift diurnal variations at 300 km over the equator, calculated for both the M1 and M2 models, are shown in Figure 6, over Fortaleza and Huancayo, for December 1978, March 1979, and June 1979, representing the three seasons. Also in the same figure, the vertical plasma drifts inferred from Huancayo and Fortaleza ionograms as $\Delta(h'F)/\Delta t$ are shown for the same months as those used in the simulation. The mean behavior of the vertical drift diurnal variation shown in Figure 6 is in good agreement with the Jicamarca vertical drift measurements during sunspot maxima presented by Fejer et al. [1979a] and with that calculated by Heelis et al. [1974]. The drift is upward during the day, showing a maximum between 1000 LT and 1100 LT, and downward during the night, and it shows an evening prereversal enhancement.

In Figure 7 we have given emphasis to the comparison between observed and calculated vertical drifts. So, only the drifts during sunset hours for both Fortaleza and Huancayo were plotted. We can compare the simulated prereversal peak occurrence times with the ones inferred from Huancayo and Fortaleza ionograms that are shown in Figure 7 as $\Delta(h'F)/\Delta t$. It is observed that the prereversal maximum occurs earlier in December and later in June over Fortaleza. The M1 simulation gives the same relative behavior although it is only in June that the calculated and observed occurrence times of the prereversal peaks are coincident. In spite of the fact that the M2 simulation failed in producing a prereversal peak in June, over Fortaleza (the explanation for this will be given later), we can see that in this simulation the relative behavior of the prereversal maximum is maintained, that is, it occurs earlier in December and later in March. Over Huancayo the

prereversal maximum occurs earlier in June and later in December, and this feature can be seen in both observed and simulated results (right part of Figure 7) although the calculated and observed occurrence times of the prereversal peaks are not coincident. It is important to note that the calculated prereversal peak occurrence time and its seasonal trend do not change with the M1 versus the M2 simulation.

The other aspect that can be analyzed is the V_z prereversal peak amplitude. We can see from Fortaleza data reproduced in Figure 6a, as $\Delta(h'F)/\Delta t$, that the highest V_{zp} amplitude occurs in March and the lowest one in June. Using the M1 simulation we can observe that the V_{zp} amplitude in December, over Fortaleza, is greater than in March, which does not agree with observations. Over Huancayo, on the other hand, we see that the M1 simulation leads to a result with similar amplitudes in March and June, and with the lowest value in December (Figure 6b), although the observations show the highest V_{zp} amplitude in March and the lowest in June.

The E and F region peak electron densities, N_m^E and N_m^F , are the only two parameters whose variations from one month to the other and from one station to the other are taken into account in the M1 simulation. It was observed that the N_m^F variations have no significant influence on the vertical drift prereversal enhancements. So, the observed V_{zp} seasonal variations over Huancayo and Fortaleza are mainly due to the N_m^E (or integrated conductivity) variations. Therefore we can conclude that the different conductivities used in the simulation have influenced both the amplitude and the occurrence time of the vertical drift prereversal peak. In this way, from Figures 5 and 7 we can see that the later the conductivity gradient goes to zero (N_m^E reaches a constant value at night), the later the vertical drift prereversal peak occurs (June over Fortaleza and December over Huancayo). Regarding this aspect, the simulated results are in good agreement with observations. The influence of the conductivity longitudinal gradient on the V_{zp} amplitude can be summarized as follows. The V_{zp} amplitude is higher when the conductivity shows a faster longitudinal variation in the evening (December over Fortaleza and March over Huancayo) than when the conductivity longitudinal variation is slower (June over Fortaleza and December over Huancayo). The V_{zp} amplitude relative behavior simulated by the M1 model is not in agreement with the observations.

The M1 simulation indeed serves to demonstrate the influence on the F region vertical drift prereversal peak, due to the conductivity longitudinal profiles that were obtained taking into account the different magnetic declination angles

over Huancayo and Fortaleza. In order to analyze the thermospheric wind effects on the F region vertical drifts, we carried out the M2 simulation, in which the atomic oxygen number densities were derived from Jacchia's [1977] model for the three months under consideration, over Fortaleza and Huancayo. The different atomic oxygen number densities ($n(0)$) obtained from the model give rise to different thermospheric winds that are representative for each station and season. The M2 simulation results are shown in Figure 6c and 6d for a 24-hour period, and in the lower part of Figure 7 during the sunset hours.

The F region vertical drift diurnal variations calculated using the M2 simulation for December 1978 and March and June 1979 over Fortaleza are shown in Figure 6c, and the seasonal behavior of the prereversal peak is shown separately in Figure 7. In this simulation the highest thermospheric winds over Fortaleza are obtained in March, with lower values in December and June. The calculated amplitude relative behavior of the F region vertical drift presents a significant modification when compared with the M1 simulation results. While in the M1 simulation, in which we have used the same $n(0)$ model in the three seasons, the highest V_{zp} amplitude had been obtained in December, in the M2 simulation the highest values are observed in March. On the other hand, the June V_{zp} amplitude was already low in the M1 simulation, and thus the lowest thermospheric wind used for June in the M2 simulation as well was insufficient to produce any significant amplitude for the V_z prereversal peak. Nevertheless the observed relative V_{zp} amplitude seasonal behavior (V_{zp} in March $>$ V_{zp} in December $>$ V_{zp} in June) has been better simulated by the M2 model than by the M1, although it seems that the thermospheric wind intensity of the M2 model is, in particular, underestimated for June. It should be pointed out that the V_{zp} occurrence times obtained by the M2 model in December and March are coincident with those obtained by the M1 model for the same months. This shows that moderate (or typical) variations in $n(0)$ or thermospheric wind intensity do not influence the V_{zp} occurrence time.

The F region vertical drift diurnal variations calculated using the M2 simulation for December 1978 and March and June 1979 over Huancayo are shown in Figure 6d, and the seasonal behavior of the prereversal peak is shown separately in Figure 7. As was already observed over Fortaleza, a lower $n(0)$ (or thermospheric wind) value has resulted in lower V_{zp} amplitudes in December and June, but we note it has not altered the V_{zp} occurrence time. It seems that the thermospheric winds of the M2 model for Huancayo are underestimated in December and overestimated in June.

These discrepancies over Huancayo could be attributed in part to its departure from the geographic equator (12°S).

The conductivity longitudinal gradient (Σ') effect on the F region vertical drift prereversal peak occurrence time is illustrated in Figure 8. The V_{zp} occurrence times were obtained using four different simulations having the conductivity longitudinal gradient going to zero at different times. We can see a positive correlation between the two variables. The later the Σ' goes to zero, the later V_{zp} occurs, although this relation is not linear. As was already discussed in connection with Figures 4 and 5, the time when $\Sigma' \rightarrow 0$ (or the time when N_m^E reaches its night value, here supposed constant) depends on the sunset times over the two magnetically conjugate E layers that are coupled to the equatorial F region by magnetic field lines. The sunset times at each conjugate E layer show a seasonal variation dependent on the magnetic declination angle. Therefore the equatorial station magnetic declination angle strongly influences the V_{zp} occurrence time seasonal behavior, as was already seen in the Fortaleza and Huancayo data (Figure 4).

5. Conclusions

It became clear from the previous discussions that it is possible to simulate the equatorial F region vertical drift prereversal behavior at a given location, conveniently choosing the conductivity models and the neutral atmosphere parameters. The V_{zp} occurrence time can be obtained by choosing appropriate conductivity longitudinal gradients, with $\Sigma' \rightarrow 0$ at a time that can be derived from Figure 8. This initial procedure will result in a V_{zp} amplitude that can be modified by using the appropriate neutral atmosphere parameters. From simulations for different test winds we have observed that a 30 percent decrease in the atomic oxygen density profile causes a 50 percent decrease in the V_z amplitudes near and at the local time of the prereversal peak. On the other hand, at local times further away from the prereversal peak, the corresponding V_z reduction is less than 20 percent, and during daytime hours a small increase (of about 5 percent) is observed in V_z with decreasing $n(0)$. Therefore, the observed seasonal V_{zp} behavior over Fortaleza and Huancayo can be explained on the basis of the magnetic declination angle influences on the conjugate E layer integrated Pedersen conductivity longitudinal gradients and of the thermospheric wind seasonal variations. The asymmetry about the magnetic equator, included in the simulation, was useful to show that the V_{zp} occurrence time is

controlled by the longitudinal conductivity gradients at the conjugate E regions, through the magnetic declination angle, and that the V_{zp} amplitudes undergo the influence of both magnetic declination angle and thermospheric winds.

Acknowledgments. The Huancayo ionograms used in connection with this work were provided by the World Data Center A for Solar Terrestrial Physics. This work was partially supported by the "Fundo Nacional de Desenvolvimento Científico e Tecnológico" under contract FINEP 537/CT.

The Editor thanks H. Rishbeth and another referee for their assistance in evaluating this paper.

References

- Abdu, M. A., J. A. Bittencourt, and I. S. Batista, Magnetic declination control of the equatorial F region dynamo electric field development and spread F, J. Geophys. Res., 86, 11443, 1981.
- Balsley, B. B., Electric fields in the equatorial ionosphere: A review of techniques and measurements, J. Atmos. Terr. Phys., 35, 1035, 1973.
- Batista, I. S., Dinamo da região F equatorial: Assimetrias sazonais e longitudinais no setor Americano, Ph.D. thesis, Rep. INPE-3760-TDL/206, Inst. de Pesqui. Espaciais, São José dos Campos, S. P., Brazil, 1986.
- Bittencourt, J. A., and M. A. Abdu, A theoretical comparison between apparent and real vertical ionization drift velocities in the equatorial F region, J. Geophys. Res., 86, 2451, 1981.
- Fejer, B. G., The equatorial ionospheric electric field: A review, J. Atmos. Terr. Phys., 43, 377, 1981.
- Fejer, B. G., D. T. Farley, R. F. Woodman, and C. Calderon, Dependence of equatorial F region vertical drifts on season and solar cycle, J. Geophys. Res., 84, 5792, 1979a.
- Fejer, B. G., C. A. Gonzales, D. T. Farley, M. C. Kelley, and R. F. Woodman, Equatorial electric fields during magnetically disturbed conditions, 1, The effect of the interplanetary magnetic field, J. Geophys. Res., 84, 5797, 1979b.
- Fejer, B. G., M. F. Larsen, and D. T. Farley, Equatorial disturbance dynamo electric fields, Geophys. Res. Lett., 10, 537, 1983.
- Gonzales, C. A., M. C. Kelley, B. G. Fejer, J. F. Vickrey, and R. F. Woodman, Equatorial electric fields during magnetically disturbed conditions, 2, Implications of simultaneous auroral and equatorial measurements, J. Geophys. Res., 84, 5803, 1979.

- Gonzales, C. A., M. C. Kelley, R. A. Behnke, J. F. Vickrey, R. Wand, and J. Holt, On the latitudinal variation of the ionospheric electric field during magnetospheric disturbances, J. Geophys. Res., 88, 9135, 1983.
- Heelis, R. A., P. C. Kendall, R. J. Moffett, D. W. Windle, and H. Rishbeth, Electrical coupling of the E and F regions and its effect on F region drifts and winds, Planet. Space Sci., 22, 743, 1974.
- Jacchia, L. G., Thermospheric temperature, density, and compositions: New models, Spec. Rep. 375, Smithsonian Astrophys. Obs., Cambridge, Mass., 1977.
- Potter, D., Computational Physics, John Wiley, New York, 1973.
- Rishbeth, H., Polarization fields produced by winds in the equatorial F region, Planet. Space Sci., 19, 357, 1971.
- Rishbeth, H., Dynamics of equatorial F region, J. Atmos. Terr. Phys., 39, 1159, 1977.
- Rishbeth, H., The F region dynamo, J. Atmos. Terr. Phys., 43, 387, 1981.
- Tsunoda, R. T., Control of the seasonal and longitudinal occurrence of equatorial scintillations by the longitudinal gradient in integrated E region Pedersen conductivity, J. Geophys. Res., 90, 447, 1985.
- Woodman, R. F., Vertical drift velocities and east-west electric fields at the magnetic equator, J. Geophys. Res., 75, 6249, 1970.
- Woodman, R. F., R. G. Rastogi, and C. Calderon, Solar cycle effects on the electric fields in the equatorial ionosphere, J. Geophys. Res., 82, 5257, 1977.
- Young, D. M., Iterative Solution of Large Linear Systems, Academic, Orlando, Fla., 1971.

I. S. Batista, M. A. Abdu, and J. A. Bittencourt, Instituto de Pesquisas Espaciais, Av. dos Astronautas, 1758, Caixa Postal 515, 12201 São José dos Campos, SP, Brazil.

(Received March 27, 1986;
revised June 26, 1986;
accepted June 30, 1986.)

Copyright 1986 by the American Geophysical Union.

Paper number 6A8488.
0148-0227/86/006A-8488\$05.00

Fig. 1. Geographic and magnetic locations of Fortaleza, Huancayo, and Jicamarca included in the study.

Fig. 2. Comparison between the mean F region vertical drift measured by Jicamarca radar (solid lines) and that simultaneously inferred using Huancayo ionograms (dashed lines) for equinoxes, summer, and winter. Also shown is the mean F layer minimum virtual height (dotted lines). Jicamarca vertical drift data were taken from Woodman [1970].

Fig. 3. F region vertical drift monthly means over Huancayo (solid lines) and Fortaleza (dashed lines) inferred as $\Delta(h'F)/\Delta t$ from ionograms around sunset time.

Fig. 4. Sunset time (dotted lines) calculated on the two magnetically conjugate E regions located north and south of (a) Huancayo and (b) Fortaleza. The numbers identifying each curve give the approximate geographical latitude of the E region under consideration. The histogramlike plots represent the V_{Zp} amplitudes, and the crosses show the V_{Zp} phase monthly mean.

Fig. 5. Local time variation of the peak E region electron density used in the simulations for Huancayo and Fortaleza representing December 1978 (solid circles), March 1979 (open circles), and June 1979 (crosses).

Fig. 6. Local time variation of the vertical ion velocity at 300 km above (a and c) Fortaleza and (b and d) Huancayo for December 1978 (solid circles), March 1979 (open circles), and June 1979 (crosses). Figures 6a and 6b were obtained using the M1 simulation, and Figures 6c and 6d using the M2 simulation. Also shown in the insets are the vertical ion velocity inferred from Huancayo and Fortaleza ionograms as $\Delta(h'F)/\Delta t$ during sunset time (the horizontal time scales of the calculated and inferred vertical ion drifts are the same).

Fig. 7. Comparison between the vertical ion drifts inferred from ionograms as $\Delta(h'F)/\Delta t$ and simulated using the M1 and M2 models for Fortaleza and Huancayo.

Fig. 8. Calculated F region vertical drift peak occurrence time (times of V_{Zp}) versus the time when the conductivity longitudinal gradient (Σ') goes to zero.

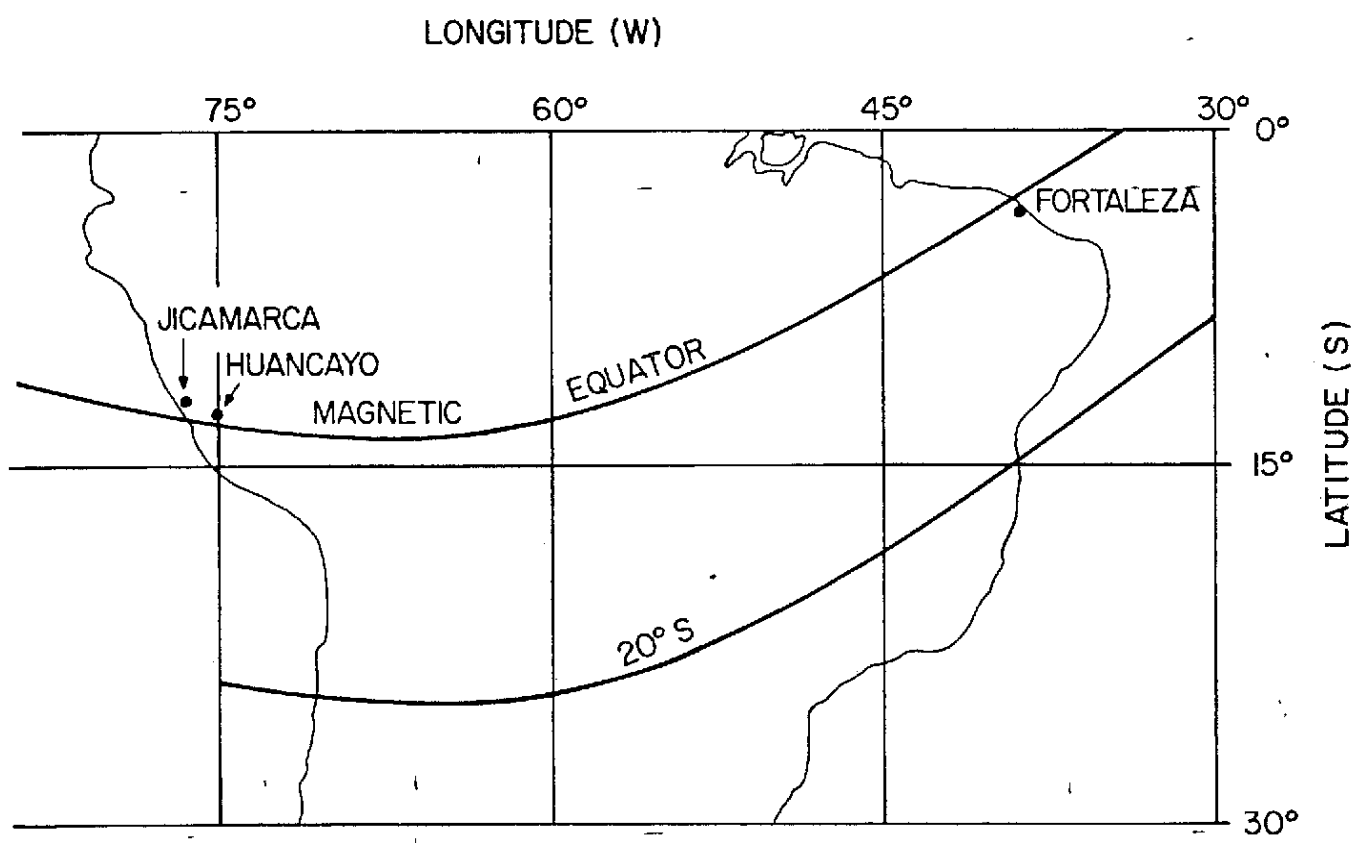


Fig. 1

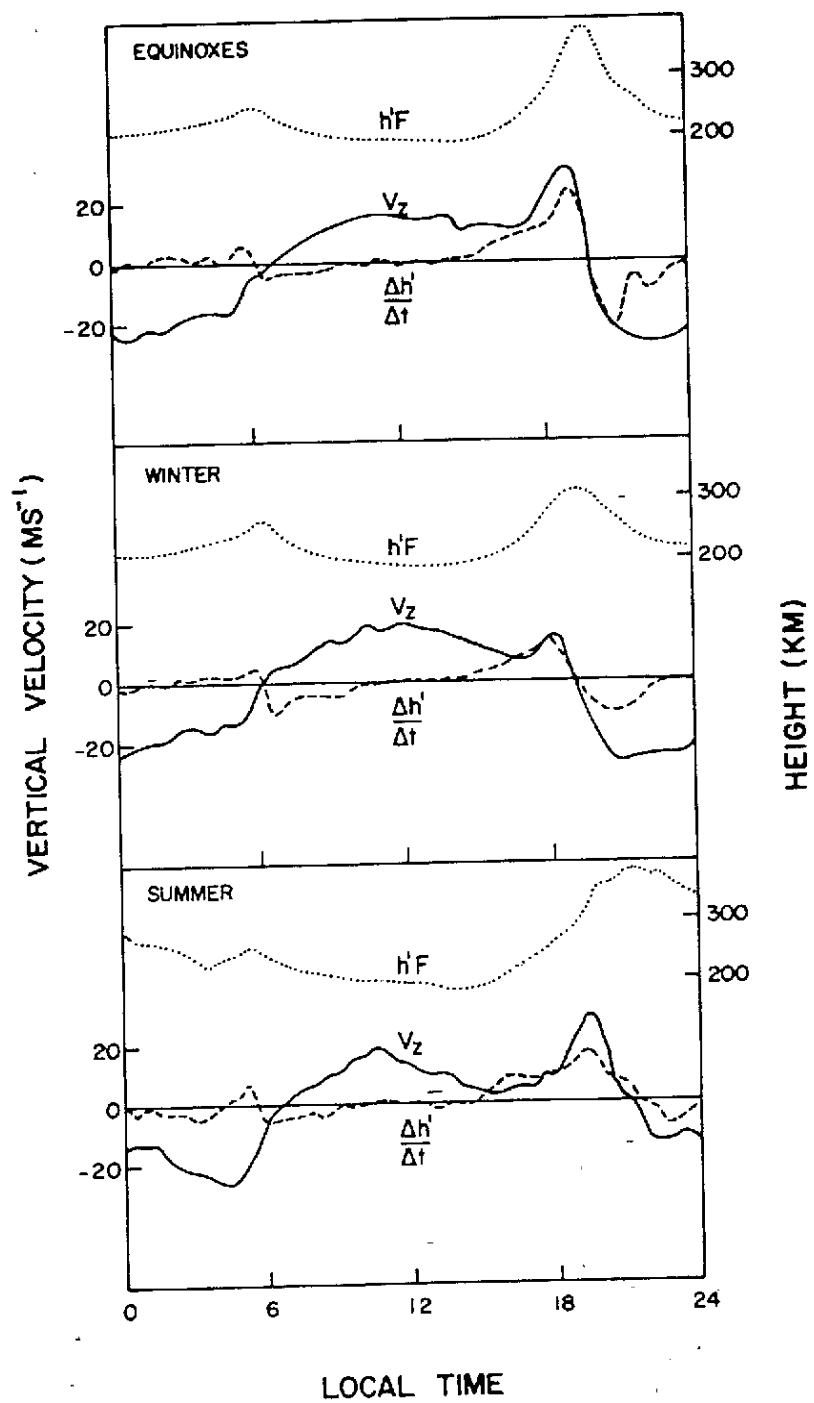


Fig. 2

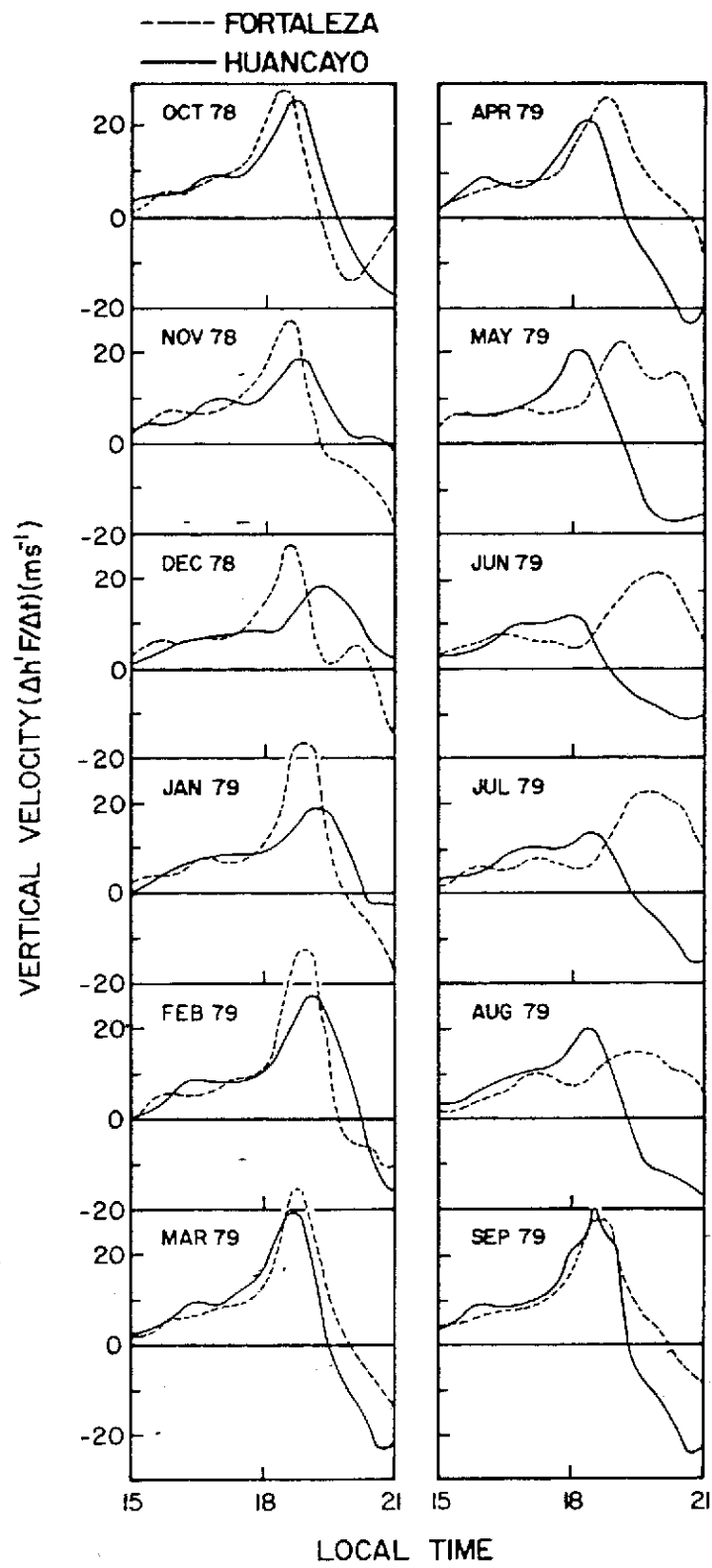


Fig. 3

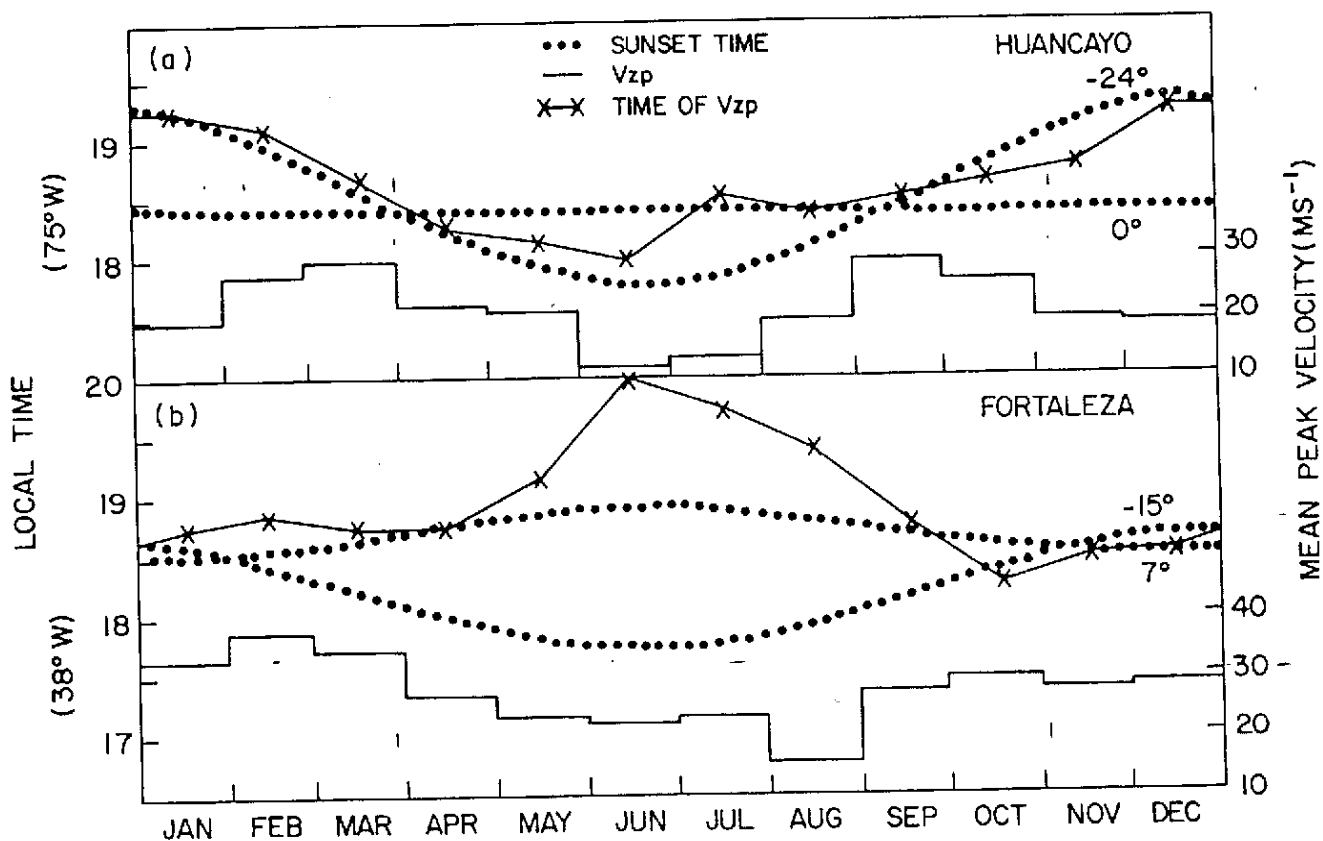


Fig. 4

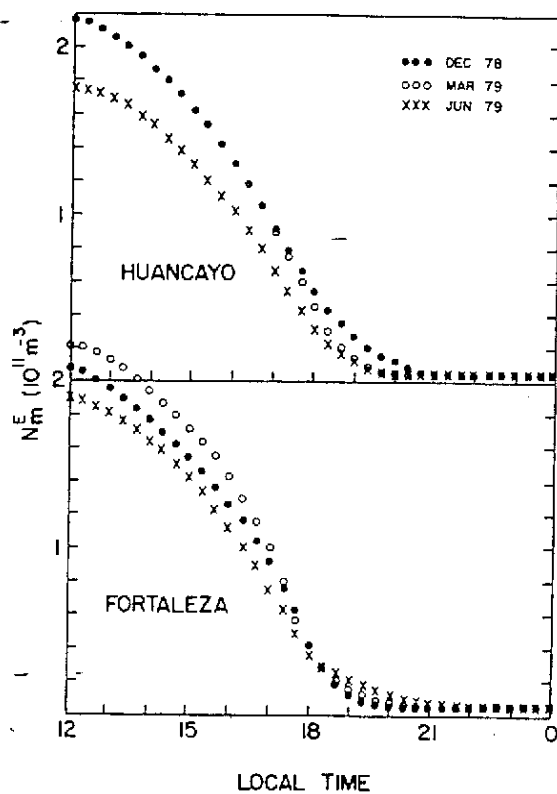


Fig. 5

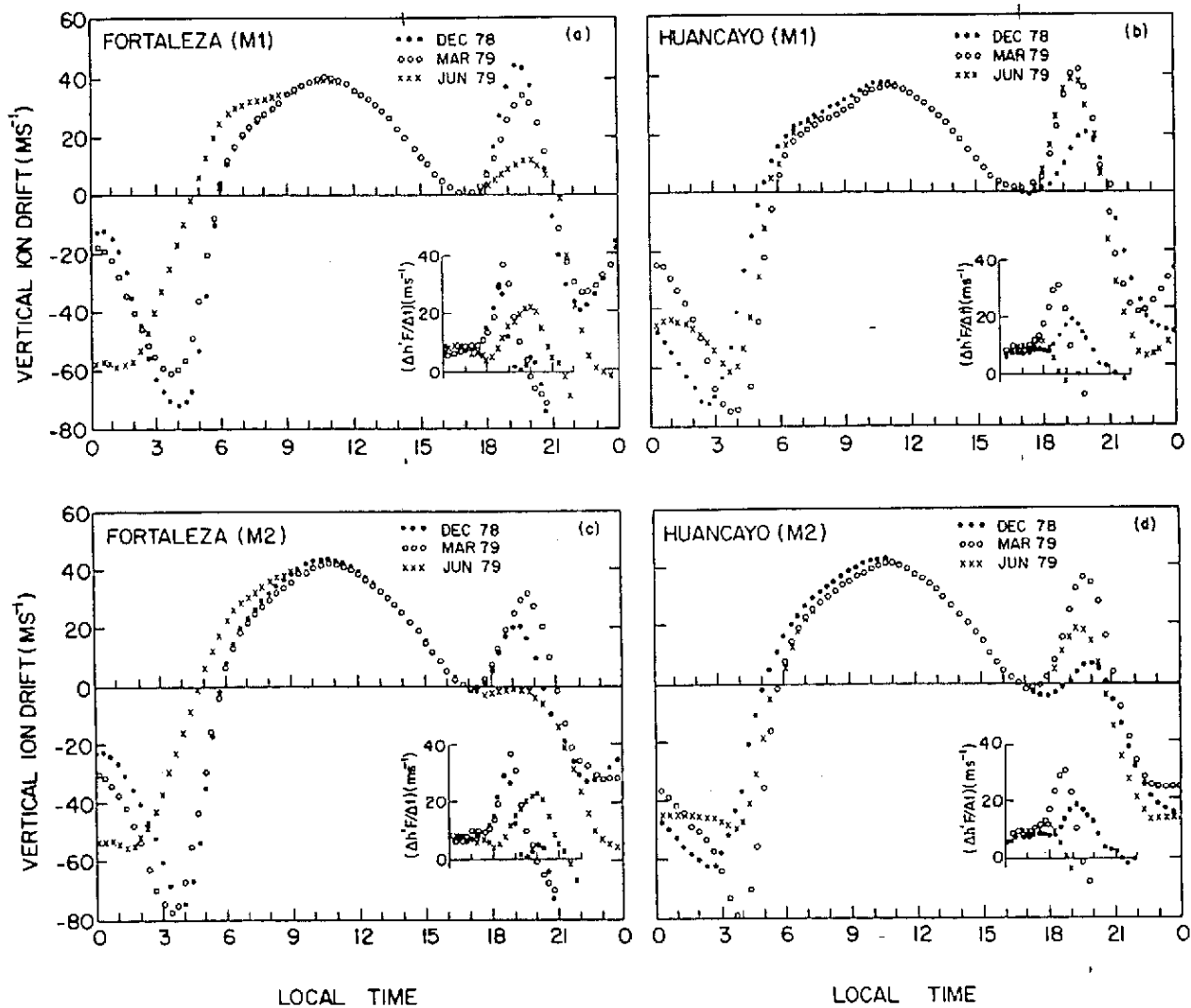


Fig. 6

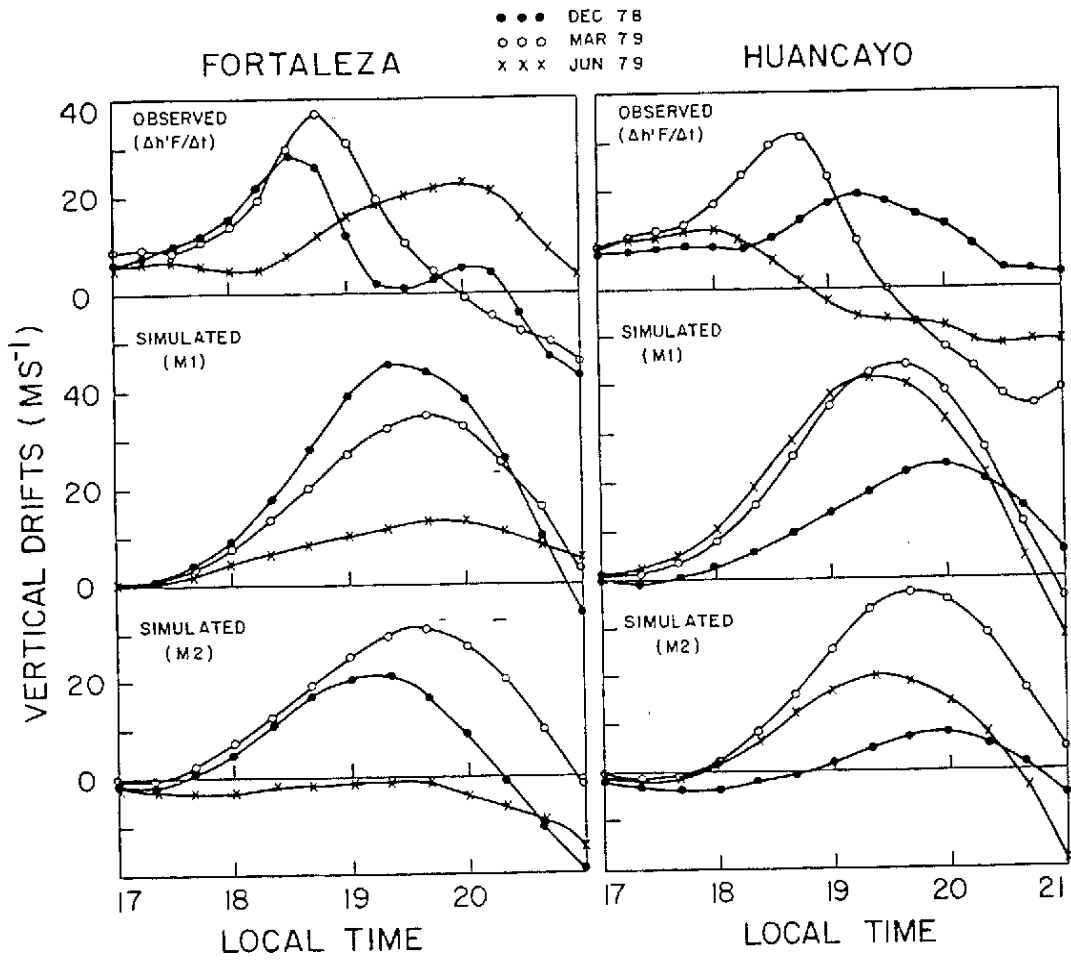


Fig. 7

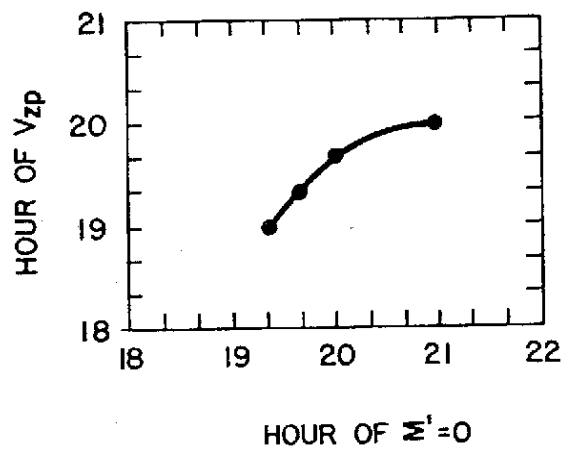


Fig. 8